frontiers in Marine Science

ORIGINAL RESEARCH
published: 16 March 2022
doi: 10.3389/fmars.2021.741536

Diversity of Pacific *Agathotanais* (Peracarida: Tanaidacea)

Anna Stępień[1], Piotr Jóźwiak[1], Aleksandra Jakiel[2], Alicja Pełczyńska[1] and Magdalena Błażewicz[1]*

[1] Department of Invertebrate Zoology and Hydrobiology, University of Łódź, Łódź, Poland, [2] Department of Genetics and Marine Biotechnology, Institute of Oceanology, Polish Academy of Sciences, Sopot, Poland

Agathotanais is one of the seven genera classified into the family Agathotanaidae. So far, 12 species have been described for the genus, seven of which are known from the Pacific. However, considering the present poor state of knowledge on deep-sea environments, a much higher number of *Agathotanais* species than currently known can be suspected. Among the studied material, collected from below 1,000 m during five deep-sea expeditions in different parts of the Pacific Ocean, we identified eight species: two of them were already known to the science and five species were identified as new to knowledge and their formal description is presented in the paper: two from the North West Pacific (the Sea of Okhotsk and Kuril-Kamchatka Trench), two from the Central Pacific (Clarion-Clipperton Fracture Zone), and one from the Australian slope. The eighth *Agathotanais* species in our material was determined using a molecular approach, but it was represented by only one partially destroyed individual and could therefore not be formally described. The proportion of *Agathotanais* collected at the Sea of Okhotsk was the highest (22%), whereas the numbers were substantially lower for the Kuril-Kamchatka Trench, and the Central and the Southern Pacific. Molecular analyses confirmed the monophyly of *Agathotanais* and *Paragathotanais* and a close relationship between both genera. Moreover, a close relationship between the two Australian species was revealed. As a result of our findings, the number of species known from the Pacific increased from 5 to 11, with the total number of species in this genus increasing from 12 to 17. An updated identification key for *Agathotanais* species is given.

Keywords: Sea of Okhotsk, Kuril-Kamchatka Trench, Clarion-Clipperton Fracture Zone, Australia, biodiversity of West and Central Pacific

OPEN ACCESS

Edited by:
Clara F. Rodrigues, University of Aveiro, Portugal

Reviewed by:
David Drumm, EcoAnalysts, Inc., United States
Andres G. Morales-Nunez, University of Maryland Eastern Shore, United States

****Correspondence:***
Anna Stępień
anna.stepien@biol.uni.lodz.pl

Specialty section:
This article was submitted to Deep-Sea Environments and Ecology, a section of the journal Frontiers in Marine Science

Received: *14 July 2021*
Accepted: *19 November 2021*
Published: *16 March 2022*

Citation:
Stępień A, Jóźwiak P, Jakiel A, Pełczyńska A and Błażewicz M (2022) Diversity of Pacific Agathotanais (Peracarida: Tanaidacea). Front. Mar. Sci. 8:741536. doi: 10.3389/fmars.2021.741536

INTRODUCTION

Genus *Agathotanais* was established to allocate *Agathotanais ingolfi* Hansen, 1913, discovered off Iceland during the *Danish Ingolf Expedition* (Hansen, 1913). It was described and marked as the most aberrant among all tanaids due to its rudimentary antenna, cheliped attached directly to the cephalothorax, the appearance of the pleopods in juvenile males (Hansen, 1913), and the setulose surface of its body (Larsen, 2005; Jóźwiak and Jakiel, 2012; Kakui and Kohtsuka, 2015). Hansen (1913) placed *Agathotanais* within the family Tanaidae Dana (1849), the only existing tanaidacean family at that time, but few decades later the *Agathotanais*, together with *Paragathotanais*, was transferred to the newly erected family Agathotanaidae Lang, 1971. The family was successively supplemented by newly erected genera and new species

(Sieg, 1986; Bird and Holdich, 1988; Błażewicz-Paszkowycz and Bamber, 2012; Jóźwiak and Jakiel, 2012). Currently, Agathotanaidae includes 54 species in seven genera, and *Agathotanais*, with 12 species, is the third genus in terms of species number after *Paranarthrura* (21 species) and *Paragathotanais* (16 species) (Hansen, 1913; Kudinova-Pasternak, 1970, 1989, 1990; Lang, 1971; Larsen, 1999, 2007; Kakui and Kohtsuka, 2015; Chim and Tong, 2021).

The history of the exploration of Pacific deep-sea regions started in the XIX century with the HMS *Challenger* expedition (1872–1876), during which the polymetallic nodules and the Mariana Trench were discovered (Schofield, 2018). Those explorations were continued for the next century aboard the RV *Vitjaz* (1949–1966), the RV *Galathea* (1951–1952), the RV *Dmitry Mendeleev* (1975–1976), or the RV *Tangaroa* (1982) (O'Hara, 2019). The regions previously considered as monotonous deserts were revealed as having a diverse topography, high nutrient densities, and a rich local diversity (Frutos et al., 2016; Golovan et al., 2018; Błażewicz et al., 2019; Washburn et al., 2021). The firsts Pacific agathotanaids described during that time (*Agathotanais splendidus* Kudinova-Pasternak, 1970, *Paranarthrura vitjazi* Kudinova-Pasternak, 1970 and *Paragathotanais zevinae* Kudinova-Pasternak, 1970) appeared as an unabundant component of macrobenthic communities, represented by several individuals only (Kudinova-Pasternak, 1970, 1983). More recently, the intensive investigation of the Pacific has applied advanced methodologies to explore the Pacific floor and trenches (Brandt and Barthel, 1995; Larsen and Shimomura, 2007; Riehl et al., 2014; Frutos et al., 2016; O'Hara et al., 2020a,b; Saeedi and Brandt, 2020; Washburn et al., 2021). As a result, six new species belonging to genus *Agathotanais* were added to the list of Pacific agathotanaids, namely: *Agathotanais hadalis* Larsen, 2007 from the North West Pacific abyssal, *Agathotanais misakiensis* Kakui and Kohtsuka, 2015 and *Agathotanais toyoshioae* Kakui and Kohtsuka, 2015 from the coast of Japan, *Agathotanais spinipoda* Larsen, 1999 from the slope of Bass Strait, and *Agathotanais manganicus* Larsen, 1999 and *Agathot*anais ahyongi Larsen, 1999 from the Central Pacific abyssal (Larsen, 1999, 2007; Kakui and Kohtsuka, 2015).

In this article, we have analyzed the new collections of the *Agathotanais* obtained from several most recent deep-sea expeditions, which explored the abyssal of the Pacific and represent the next step for discovering the variability of deep-sea tanaid diversity. Using morphological and genetic tools, we present the description of five new species of *Agathotanais* collected from four areas of the Pacific: Clarion-Clipperton Fracture Zone (two species), off East Australia (one species), the Sea of Okhotsk (one species), and the Kuril-Kamchatka Trench (KKT) (one species). We discuss their bathymetric and zoogeographical distributions. Additionally, with genetic tools, we have detected one more new species off SE Australia, that was represented by only one speciemen in poor condition. This speciem was dissected and prepared into slides. It would provide a holotype of substandard quality and therefore it is not be formally described as a named species in this article.

MATERIALS AND METHODS

Sampling

A total of 738 specimens of the genus *Agathotanais* were collected from from five deep-sea projects (**Supplementary Table 1**).

1. A total of 634 specimens were collected in the Sea of Okhotsk during the German-Russian expedition SokhoBio (Sea of Okhotsk Biodiversity Studies) aboard the RV *Academic M.A. Lavrentyev* between July and August of 2015 (Malyutina et al., 2015). Specimens of *Agathotanais* were found in twelve epibenthic sledge (EBS) samples.
2. A total of 70 specimens were collected in the KKT and the adjacent abyssal zone during two expeditions: KuramBio (Kuril-Kamchatka Biodiversity Study, NW Pacific abyssal, and western KKT slope) and KuramBio II (KKT slope) in 2012 and 2016, respectively aboard the RV *Sonne*. *Agathotanais* was present in 12 EBS samples taken during KuramBio and KuramBio II.
3. A total of 21 specimens were collected in 2015 in the Central Pacific (Clarion-Clipperton Fracture Zone, CCZ) during the EcoResponse (SO-239) cruise, one of the Joint Project Initiative Oceans (JPIO) expeditions. From a total of eleven EBS deployments, *Agathotanais* was found in the following License Areas: Bundesanstalt fur Geowissenschalfen und Rofstoffe (BGR, Germany); Interoceanometal Joint Organisation (IOM); Global Sea Mineral Resources NV, Belgium (GSR); Areas of Particular Environmental Interest 3 (APEI3).
4. Five specimens were collected off the SE Australian coast during the ABYSS (Sampling the Abyss) expedition in 2017 from aboard the RV *Investigator*. *Agathotanais* were found in three EBS samples.
5. Two specimens collected in the continental slope off SE Australia, during the SLOPE campaign in 1988 and 1994. *Agathotanais* was found in two samples collected by dredging.

Except for the SLOPE collection that was preserved in formalin, all specimens were fixed in 96% ethanol. Specimens from the Sea of Okhotsk, the KKT, and Central Pacific have been loaned from the Zoological Museum Hamburg (ZMH), Natural History Museum in Frankfurt (NHM) and A.V. Zhirmunsky National Scientific Center of Marine Biology in Vladivostok (MIMB). Material from the Australian and Tasmanian coast has been loaned from the Museum Victoria in Melbourne (catalog numbers start with J and NMV).

Phylogenetic and Genetic Distance Analyses

The analyses included 16 specimens from the Sea of Okhotsk (SokhoBio collection), 16 from the KKT (KuramBio collection), 21 from the Central Pacific (JPIO collection), and two specimens from Australia (ABYSS collection). For the DNA extraction, the whole specimen was taken as starting material using sterile needles and following the Chelex (InstaGene Matrix, Bio-Rad) method as in Palero et al. (2010). The ribosomal RNA18S and

the histone H3 genes were amplified using a 25 μl-volume reaction containing 13 μl AccuStart II GelTrack PCR SuperMix, 10 μl H_2O, 0.5 μl of each primer (10 pmol/μl) and 2 μL DNA template. The 18S fragments were amplified using the universal primers SSU_F04 and SSU_R22 (Blaxter et al., 1998) following the protocol: 95°C for 2 min, 95°C for 1 min, 57°C for 45 s, 72°C for 3 min, for 35 cycles, and a final elongation of 10 min at 72°C. The H3AF and H3AR fragments (Colgan et al., 1998) were obtained according to the protocol: 95°C for 3 min, 95°C for 30 s, 50°C for 30 s, 72°C for 1 min, for 35 cycles, and a final elongation of 15 min at 72°C. A 2 μl-aliquot of the PCR product was visualized in a Midori Green-stained (Nippon Genetics) 1.5% agarose gel to verify its quality and length. PCR purification and sequencing using forward and reverse primers were carried out by MACROGEN (Amsterdam, Netherlands). Consensus sequences were built using Geneious version 9.1.3[1] and compared with the GenBank database with BLAST (basic local alignment search tool, NCBI) (Altschul et al., 1990) to discard contamination from non-arthropod sources. Sequences were aligned using the option L-INSi of MAFFT (multiple alignment using fast Fourier transform) (Katoh and Standley, 2013), as implemented in Geneious. Genetic distances were calculated using pairwise distances and run-on *p*-distance model using MEGA 7 (Molecular Evolutionary Genetics Analysis, Pennsylvania State University) (Kumar et al., 2018). Before running molecular phylogenetic analyses, the most suitable nucleotide substitution model was selected according to the AICc (The Akaike information criterion) and BIC (the Bayesian information criterion) criteria as implemented in MEGA 7 (Kumar et al., 2018). The aligned sequences and selected evolutionary model were then used to obtain a Maximum Likelihood phylogenetic tree in BEAST (BEAST Developers) (Drummond et al., 2012). Node support was evaluated with, bootstrap replicates. MCMC (Markov chain Monte Carlo) analyses were set for 10 million generations whereas all Effective Sample Size (ESS) values were calculated with Trace Analysis Tool (Tracer v1.5.0) software (Rambaut et al., 2018). To analyze the MCMC outputs Tree Annotator v1.7.5 (Drummond and Rambaut, 2007) was used with the default parameters.

Species Description

Chemically sharpened tungsten needles were used for the dissection of the individuals selected for detailed morphological analyses. The dissected appendages were placed on a microscope slide on a drop of glycerine, protected with a cover glass, and sealed with a ring of melted paraffin (Błażewicz et al., 2021). Drawings were prepared using a light microscope (Nikon Eclipse 50*i*, Japan) equipped with a *camera lucida*. Publication-quality illustrations were prepared using a digital tablet and Adobe Illustrator (Adobe inc.) (Coleman, 2003). Total body length (BL) was measured along the main axis of symmetry from the frontal margin to the end of the telson. Body width (BW) was measured at the widest point along the main axis of symmetry. The measurements of specimens were made with the help of a camera connected to the microscope (Nikon Eclipse Ci-L) using NIS-Elements View software[2]. The morphological description follows Jakiel et al. (2019), where the expression '*N*x' replaces '*N* times as long as' and '*N* L:W' replaces '*N* times as long as wide.'

For appendage ornamentation, we have followed the classification according to Garm and Watling (2013). Following types were used: (1) simple setae; (2) plumose setae; (3) serrated setae; (4) setules; (5) spines. For more specific ornamentation we used the following definition: (6) penicillate seta – with a tuft of setules located distally and with a small knob on which a seta is fixed to the tegument; and (7) spinule – short, tiny spine.

The stages recognized among the studied individuals were: manca (II and III), neuter, and a juvenile male. Specifically, the term 'manca' describes juveniles with (manca III) or without (manca II) buds on pereopod-6. 'Neuter' is retained for the development stage after manca that cannot be classified as either female or juvenile male. Juvenile male refers to individuals with initially developed pleopods.

Confocal Laser Scanning Microscopy

Two individuals from the SokhoBio collection (neuter: ZMH K-61187, juvenile male: ZMH K-61184) and two individuals from the KuramBio collection (neuter: ZMH K-61178) were used for imaging. Pictures were obtained with a confocal laser scanning microscope CLSM 780 (Zeiss) equipped with a Plan-Apochromat 10x/0.47 M27 objective and the InTune tunable excitation laser system (set to excitation at wavelength 555 nm).

Ethanol-preserved specimens were stained for 48 h with a mixture of equal volumes of saturated aqueous solutions of Congo red and acid fuchsin. Animals were sequentially washed in 80% glycerol and 100% glycerol and kept in 100% glycerol. Fluorescence was registered in the emission range 560–696 nm. Scan images were collected for further editing. Images were pseudo-colored in gold and reconstructed into a 2D stack image with maximum intensity projection using ZEN 2012 (Zeiss).

Scanning Electron Microscopy

One individual from the SokhoBio material (neuter: ZMH K-61187) and two individuals from the Clarion-Clipperton Fracture Zone material (neuter: ZMH-K-61146, neuter: ZMH-K-61156) were used for imaging with a Phenom ProX microscope. Specimens for the scanning electron microscopy analysis were initially rinsed with distilled water to remove the ethanol from their surface and tissues and then transferred to the SEM stub mounted in a temperature-controlled sample holder and frozen at –10°C.

RESULTS

Diversity, Abundance, and Distribution

A total of 736 specimens of *Agathotanais* were classified into eight species, five of which were new to science: *A. beatae* n. sp., *A. frutosae* n. sp. *A. jani* n. sp., *A. oharai* n. sp., *A. paleroi* n. sp. One of the species was represented by only one individual as was

[1] www.geneious.com

[2] www.nikoninstruments.com

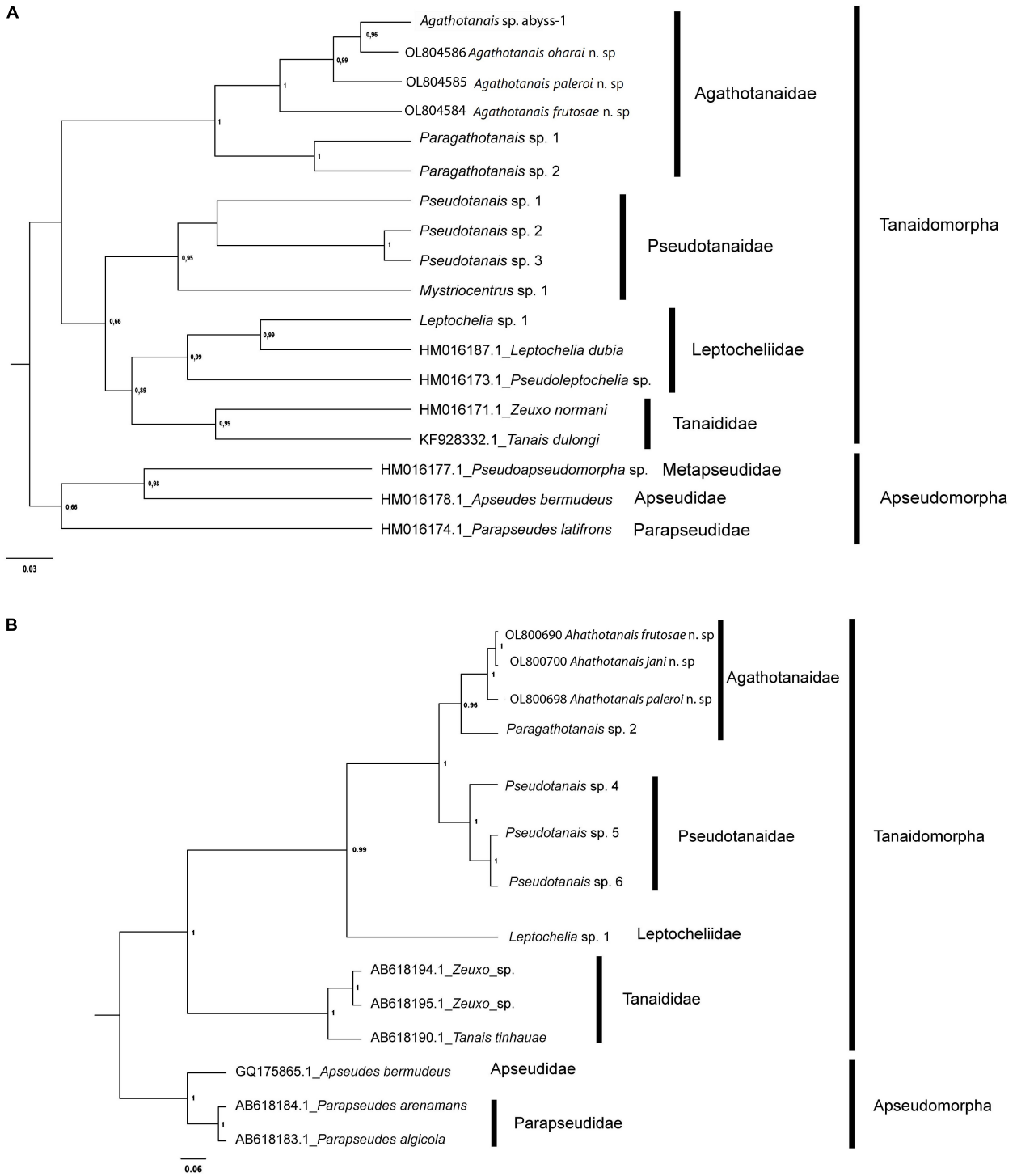

FIGURE 1 | Evolutionary relationships of Agathotanaidae species inferred by using the Histone H3 **(A)** and 18S **(B)** sequences and the Maximum Likelihood method. The percentage of trees in which the associated taxa clustered together (bootstrap support) is shown next to the branches. Only values above 0.6 are shown.

not formally described (*Agathotanais* sp. abyss-1). Only two of the sampled species: *A. hadalis* and *A. spinipoda*, from the Japan Trench (NW Pacific) and the SE Australian Slope, respectively, were already known (Larsen, 1999, 2007).

Most of the species studied here were represented by several specimens. However, *A. frutosae* was extremely abundant in the Sea of Okhotsk, represented by 634 specimens. The majority of them were found in the Kuril Basin, the deepest part of the Sea,

and only ten specimens were collected on the outer slope of Kuril Island (st. 9-7). In the KKT and the adjacent abyssal, we have recorded two species. One of them, *A. hadalis*, was identified on the basis of only three specimens, but *A. paleroi*, was relatively abundant and represented by 67 specimens that were all collected from the western side of the KKT, except for one specimen, found on the eastern side (st. 3-9). In the Central Pacific (CCZ), *Agathotanais* was represented by 21 specimens: four of them were identified as *A. beatae* and 17 as *A. jani*. Finally, six individuals were found off the Australian coast: two specimens were assigned to the species *A. spinipoda*, three to *A. oharai,* and one was classified as *Agathotanais* sp. abyss-1.

Phylogenetic and Genetic Distance Analysis

A total of four H3 and three 18S different haplotypes were obtained (**Figure 1**), representing *Agathotanais* species. The sequence alignments spanned 298 bp for H3 and 550 bp for 18S. For H3 the Kimura 2-parameter (K2+G+I) model showed the lowest AICc (AICc = 3614.52) and BIC (BIC = 3837.83) scores. The non-uniformity of evolutionary rates among sites was modeled using a Gamma distribution (+G = 1.39). The rate variation model revealed that some positions were evolutionarily invariable (+I = 44% sites). The Maximum Likelihood tree with the highest log-likelihood value (lnL = –1,770.90) was obtained.

For 18S the Kimura 2-parameter (K2+G) model showed the lowest AICc (AICc = 1313.07) and BIC (BIC = 1475.82) scores, which is considered to describe the best substitution pattern. Non-uniformity of evolutionary rates among sites was modeled using a Gamma distribution (+G = 0.32). The Maximum Likelihood tree with the highest log-likelihood value (lnL = –624.84) is shown in **Figure 1**.

All *Agathotanais* species included in the analyses were grouped into a well-supported clade. Additionally, the genetic clustering in the ML trees of the obtained haplotypes agrees with the morphological identification of taxa (see below).

The pairwise genetic p-distances between all the agathotanaid specimens ranged between 5.4 and 17.4% for H3, while for 18S sequences they ranged between 1 and 4% (**Supplementary Table 2**). The intraspecific genetic variation was very low, as expected given the limited sample size per species, represented in all cases by one haplotype for both markers. The evolutionary divergences for sequence pairs for H3 were largest between *A. frutosae* and both Australian species (*A. frutosae* – *Agathotanais* sp. abyss-1 1.174 ± 0.023 and *A. frutosae* – *A. oharai* 0.161 ± 0.022), while the lowest divergences were observed between *Agathotanais* sp. abyss and *A. oharai* (0.054 ± 0.012). Divergences between 18S sequences are shown in **Supplementary Table 2**.

Taxonomic Description

Genus: *Agathotanais* Lang, 1971

Diagnosis (amended after Larsen, 2005). Body strongly calcified, with a pitted surface. Pleon narrower or similar in width to pereon or pleotelson. Antennule with three articles. The antenna is usually one-articled (except *A. manganicus* antenna two-articled). The mandible molar process conical, left mandible *lacinia mobilis* is absent or reduced. Labium with the spiniform distal process and lateral process. Maxilliped bases partially fused. Cheliped slender, attached ventrally to cephalotorax, carpal sclerite absent (basal lobe truncated). Marsupium (where known) with four pairs of oostegistes. Pereopod coxa present. Uropods short, exopod reduced and fused with the basal article, endopod one- or two-articled. All appendages are covered with dense setules apart from the distal part of cheliped and pereopod dactyli.

Species included: *Agathotanais ahyongi* Larsen, 1999, *A. beatae* **n. sp.**, *A. brevis* Kudinova-Pasternak, 1990, *A. cilacapicus* Chim and Tong, 2021, *A. frutosae* **n. sp.**, *A. ghilarovi* Kudinova-Pasternak, 1989, *A. hadalis* Larsen, 2007, *A.* hanseni Lang, 1971, *A. ingolfi* Hansen, 1913, *A. jani* **n. sp.**, *A. manganicus* Larsen, 1999, *A. misakiensis* Kakui and Kohtsuka, 2015, *A. oharai* **n. sp.**, *A. paleroi* **n. sp.**, *A. spinipoda* Larsen, 1999, *A. splendidus* Kudinova-Pasternak, 1970, *A. toyoshioae* Kakui and Kohtsuka, 2015.

Agathotanais hadalis Larsen, 2007

Material examined: Juvenile male, broken, KuramBio st. 2-10, (NHM 58020); neuter, broken, KuramBio st. 8-1, (NHM 58021).

Distribution: Kuril-Kamchatka Trench (**Figure 2**); depth range 4700–5700 m.

Agathotanais spinipoda Larsen, 1999

Material examined: Neuter, broken, SLOPE st. 134, (NMV J61570); neuter, broken, SLOPE st. 62 (NMV J68224).

Distribution: Bass Strait Slope (SE Australia) (**Figure 2**); depth range 400–1840 m.

Agathotanais beatae **n. sp. Jóźwiak and Pełczyńska**.

This species is register under the zoobank number: urn:lsid:zoobank.org:act:26601B4E-AEBA-4C15-9EFC-35A664309F8F

(**Figures 3**, **4**)

Material examined: Holotype: neuter, 3.3 mm, JPIO st. 96, (ZMH-K-61146).

Paratypes: neuter, 3.1 mm, dissected on slides, JPIO st. 158, (ZMH-K-61147); neuter, damaged, JPIO st. 24, (ZMH-K-61148).

Diagnosis of neuter: Body narrow (about 11 L:W). Carapace without lateral setae in posterior margin. Pereonite-1 without pair of dorsal setae. Pereonites 4–6 longer than wide. Pereonite-6 1.5× pleonites 1–5 combined. The pleonites 1–5 width subequal to pereonite-6. Antennule article-1 longer than the remaining articles combined, about 2.0× article-3. Antenna one-articled. Cheliped palm 1.3 L:W. Pereopods 2–3 carpus dorsodistal seta 0.4× propodus. Pereopods 4–6 unguis serrated, but without distinct, pointed teeth ventrally. Uropod endopod one-articled.

Etymology: Species is named after Mrs. Beata Pełczyńska, mother of AP.

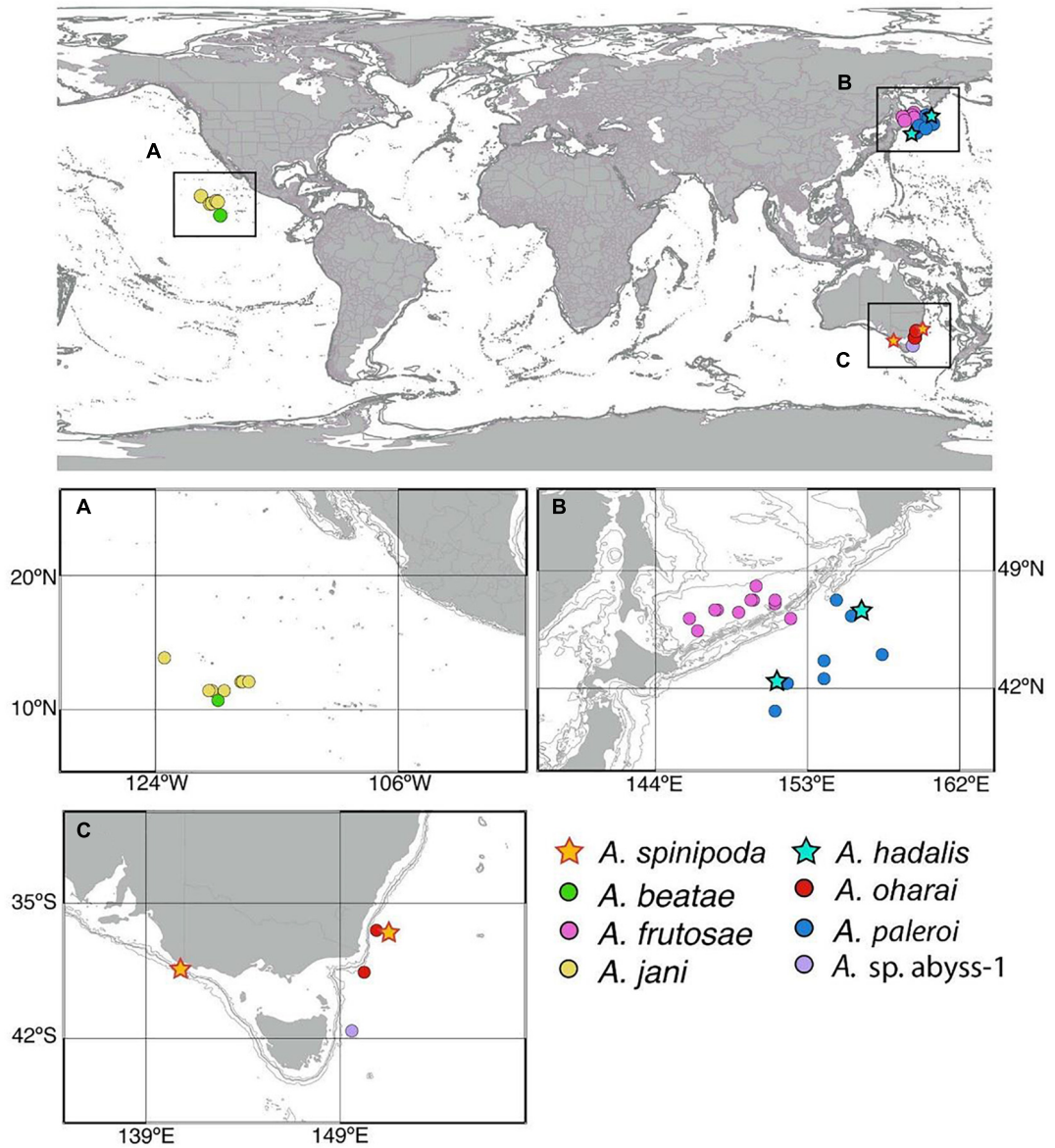

FIGURE 2 | Distribution of new species of *Agathotanais* collected from central Pacific **(A)**, Sea of Okhotsk, Kuril-Kamchatka Trench (KKT) **(B)**, and along Australian coast **(C)**.

Description of neuter: Body from the holotype (ICUL1786), appendages from the paratype (ICUL10315). BL = 3.4 mm. Body (**Figures 3A,B**) 10.5 L:W, cylindrical and elongated. Carapace 1.2 L:W, 0.2× BL. Pereon 0.8× BL. Pereonites 1–6: 0.7, 1.0, 1.0, 1.3, 1.6, and 1.3 L:W, respectively. Pleon with pleotelson 0.1× BL. Pleonites 1–5 0.2 L:W each. Pleotelson dorsally almost as long as pleonites 2–5 combined, acorn-shaped in the dorsal view, apex blunt, pointed, directed backward.

Antennule (**Figure 3C**) article-1 3.7 L:W, 4.2× article-2, with five penicillate midinner setae, three penicillate subdistal setae and two short and one penicillate distal setae; article-2 1.3 L:W, 0.5× article-3, with two subdistal setae: one inner and one outer; article-3 3.4 L:W, with six simple setae, one penicillate seta, and one aesthetasc.

Antenna (**Figure 3D**) one-articled, 3.0 L:W, tipped with a short distal seta.

Mouthparts: Right mandible (**Figures 3E,E'**) incisor broad and smooth.

Left mandible (**Figure 3F**) incisor with three teeth; *lacinia mobilis* narrow, rounded.

Maxillule endite (**Figure 3G**) with eight distal spines.

Labrum (**Figure 3H**) rounded, densely covered with setae of different lengths.

Maxilliped (**Figure 3I**) palp article-1 1.4 L:W, naked; article-2 1.3 L:W, with two inner plumose setae; article-3 2.4 L:W, with

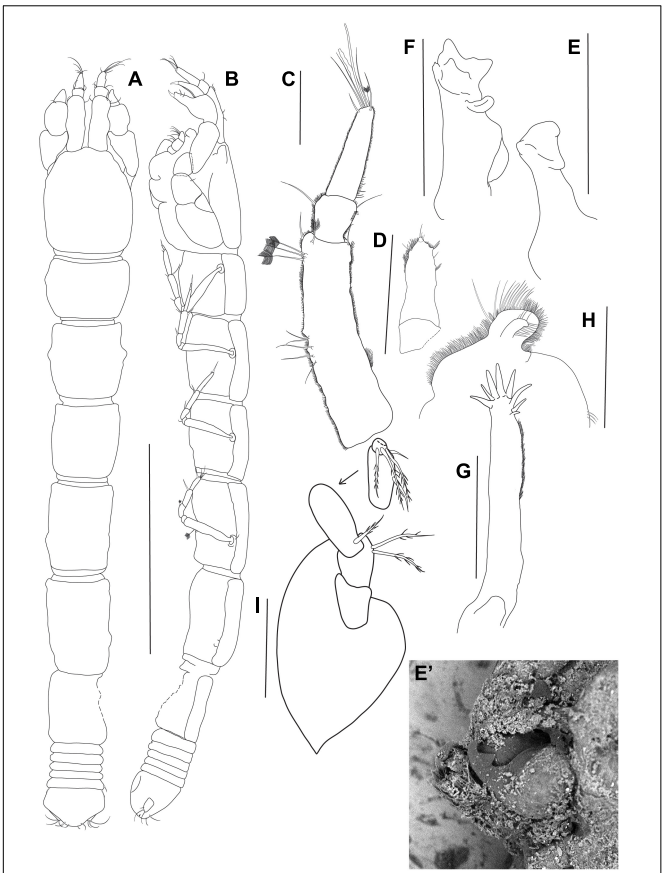

FIGURE 3 | *Agathotanais beatae* n. sp., neuter, holotype (**A,B**: ZMH-K-61146; **C–I** ZMH-K-61147). **(A)** dorsal view; **(B)** lateral view; **(C)** antennule; **(D)** antenna; **(E)** right mandible; **(E')** details of right mandible (SEM image); **(F)** left mandible; **(G)** maxillule; **(H)** labrum; **(I)** maxilliped. Scale bars: **(A,B)** = 1 mm, **(C–I)** = 10 μm.

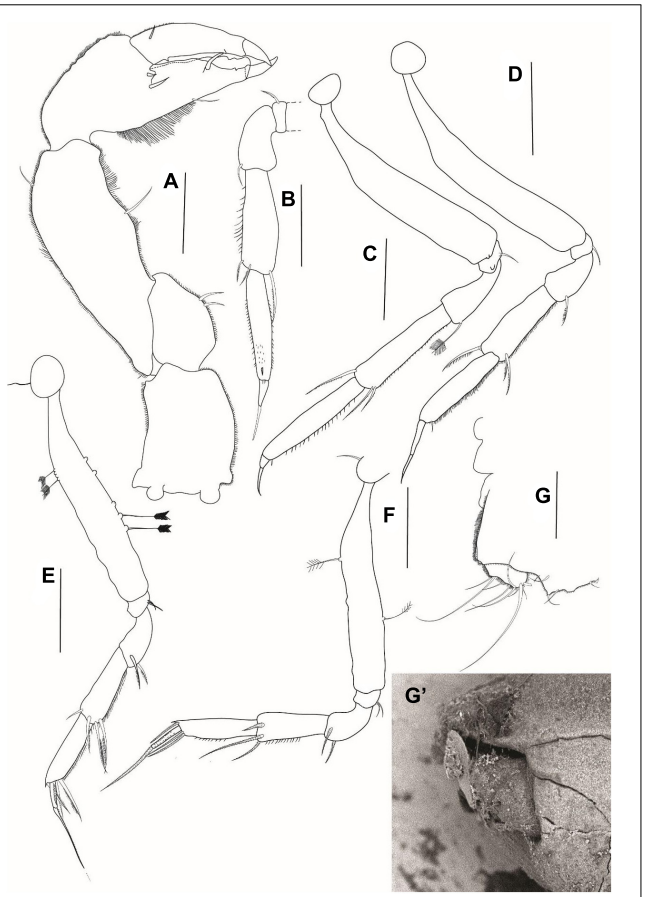

FIGURE 4 | *Agathotanais beatae* n. sp., neuter, holotype (ZMH-K-61146). **(A)** cheliped; **(B)** pereopod-1; **(C)** pereopod-2; **(D)** pereopod-3; **(E)** peropod-5; **(F)** peropod-6; **(G)** uropod; **(G')** detail of uropod (SEM image). Scale bar: **(A–G)** = 100 μm.

plumose proximal seta and two inner setae; article-4 2.2 L:W, with three plumose distal setae. Basis margins rounded.

Cheliped (**Figure 4A**) basis 1.5 L:W, naked; merus with two midventral setae; carpus 2.6 L:W, slightly shorter than propodus and fixed finger combined, with one midventral and one dorsodistal setae; palm 1.3 L:W, with two short spines near dactylus insertion, fixed finger subequal palm, with ventral seta and numerous long setules, cutting margin irregular, with one seta visible, terminal spine large and sharp; dactylus as long as fixed finger, with short dorsoproximal seta, cutting margin with two teeth; unguis robust and sharp.

Pereopod-1 (**Figure 4B**) basis damaged; ischium with ventrodistal seta; merus 2.0 L:W, 0.6× carpus, with ventrodistal seta; carpus 3.0 L:W, 0.9× propodus, with two serrated ventrodistal and one serrated dorsodistal (0.4× propodus) setae; propodus 5.0 L:W, 4.1× dactylus and unguis combined, with ventrodistal minute spine; dactylus 3.4 L:W, 0.8× unguis; dactylus and unguis unarmed, unguis with a tip pointed.

Pereopod-2 (**Figure 4C**) coxa naked; basis 5.7 L:W, naked; ischium with ventrodistal seta; merus 2.4 L:W, 0.6× carpus, with penicillate ventrodistal seta; carpus 4.5 L:W, 0.9× propodus, with three serrated setae: two ventrodistal and one dorsodistal (0.4× propodus); propodus 5.4 L:W and 4.5× dactylus and unguis combined, with small ventrodistal seta; dactylus 3.4 L:W, 0.8× unguis, unarmed; unguis unarmed with a pointed tip.

Pereopod-3 (**Figure 4D**) coxa naked; basis 8.0 L:W, naked; ischium with ventrodistal seta; merus 1.9 L:W, 0.6× carpus, with serrated ventrodistal seta; carpus 3.0 L:W, 0.8× propodus, with three serrated setae: two ventrodistal and one dorsodistal (0.4× propodus); propodus 4.6 L:W and 3.2× dactylus and unguis combined, with short ventrodistal seta; dactylus 5.0 L:W, 0.5× unguis, unarmed; unguis unarmed with a pointed tip.

Pereopod-4 (**Figure 4E**) coxa with seta; basis 6.0 L:W, with two penicillate dorsal setae, and five penicillate ventral setae (some setae broken); ischium with two ventrodistal setae; merus 1.4 L:W, 0.5× carpus, with two serrated ventrodistal setae; carpus 2.9 L:W, 1.1× propodus, with two serrated ventrodistal setae, one serrated subdistal seta, and one dorsodistal seta; propodus 4.2 L:W, 2.9× dactylus and unguis combined, with two serrated ventrodistal setae and one serrated dorsodistal seta; dactylus 4.2 L:W, 0.4× unguis, ventrally serrated; unguis ventrally serrated, with a pointed tip.

Pereopod-5 was damaged in the dissected specimen, but in other individuals like pereopod-4.

Pereopod-6 (**Figure 4F**) coxa with seta; basis 6.6 L:W, with one middorsal and one midventral penicillate setae; ischium with two ventrodistal setae; merus 1.7 L:W, 0.6× carpus, with two serrated ventrodistal setae; carpus 2.6 L:W, 0.9× propodus, with two serrated ventrodistal setae and one serrated dorsodistal seta; propodus 3.7 L:W and 2.2× dactylus and unguis combined, with three serrated distal setae; dactylus 6.0 L:W, 0.5× unguis; unguis ventrally serrated, with a pointed tip.

Uropod (**Figures 4G,G'**) exopod reduced and fused with the basal article; endopod one-articled, with two lateral setae and five distal setae on terminal segment.

Distribution: Central Pacific, Clarion-Clipperton Fracture Zone, IOM (**Figure 2**); depth: 4418 m.

Remarks. One-articled antenna distinguishes *A. beatae* n. sp. from *A. ahyongi* and *A. manganicus*, which have a fully reduced or two-articled antenna, respectively (Larsen, 1999). Pereonites 4–5 longer than wide allow to separate *A. beatae* from *A. brevis* having those pereonites wider than long (Kudinova-Pasternak, 1990), and *A. ingolfi* that has these pereonites subequal in length (Hansen, 1913). A longer than wide pereonite-6 differentiates *A. beatae* from *A. hadalis*, *A. frutosae*, *A. paleroi*, and *A. spinipoda*, which have the pereonite-6 as long as wide (*A. frutosae*, *A. paleroi*, and *A. spinipoda*) or clearly wider than long (*A. hadalis*).

A relatively long article-3 in antennule (about 0.5× article-1) distinguishes *A. beatae* from *A. splendidus*, and *A. toyoshiae*. In these two species the length of article-3 is about 0.3× article-1 (Kudinova-Pasternak, 1970; Kakui and Kohtsuka, 2015). A serrated ventral margin of the unguis in pereopods 4–6 separates *A. beatae* from *A. ghilarovi*, *A. hanseni*, *A. oharai*, and *Agathotanais* sp. abyss-1, for which the unguis is unarmed (Lang, 1971; Kudinova-Pasternak, 1989), and from *A. jani* which has two or three distinct teeth on the unguis. Furthermore, the new species differs from *A. misakiensis* by having a carapace shorter than the combined length of the two succeeding pereonites (for *A. misakensis* the carapace is subequal to pereonites 1–2). A two-articled uropodal endopod observed in *A. cilacapicus* separates this species from *A. beatae* that has a one-articled uropod (**Table 1**).

***Agathotanais frutosae* n. sp. Stępień, Jakiel, and Błażewicz.**

This species is register under the zoobank number: LSIDurn:lsid:zoobank.org:act:E07E39AE-D3ED-4128-B8F9-CA4194A05496

(**Figures 5–7**)

Material examined: Holotype: neuter, 3 mm, SokhoBio st. 7-4, (NHM 58033).

Paratypes: neuter, dissected on slides, 2.9 mm, SokhoBio st. 7-4, (NHM 58034); neuter, 3.1 mm, dissected on slide, SokhoBio st. 11-6, (NHM 58035); juvenile male, 3 mm, SokhoBio st. 2-7, (ZMH K-61184) juvenile male, dissected on slides, 2.6 mm, SokhoBio st. 11-6, (ZMH K-61183); seven juvenile males, 2.1–2.6 mm, SokhoBio st. 7-4, (ZMH K-61185); four neuters, 2.7–3.3 mm, SokhoBio st. 9-7, (ZMH K-61186); two neuters, 2.8–3.2 mm, SokhoBio st. 9-7, (NHM 58036); manca III, 1.8 mm,

TABLE 1 | Diagnostic features distinguishing the species of *Agathotanais*: (1) Pereonites 4–5 L:W; (2) Pereonite-6 L:W; (3) Pleon: pereonite-6; (4) Antennule article-3:article-1; (5) Antenna numbers of articles; (6) Maxilliped endites distal denticles; (7) Cheliped palm L:W; (8) Fixed finger number of setae; (9) Pereopod-2 dorsodistal carpal seta: propodus length; (10) Pereopod-3 dorsodistal carpal seta length: propodus; (11) Pereopod-4 propodus row of small spines; (12) Pereopods 4–6 dactylus small accessory spine; (13) Pereopods 4–6 unguis ventral ornamentation; (14) Uropod endopod number of articles.

Species/features	1	2	3	4	5	6	7	8	9	10	11	12	13	14
A. ahyongi	Longer	Longer	Narrower	0.6	0	Absent	1.6	1?	0.1	0.1	Absent	Absent	Unarmed	One
***A. beatae* n. sp.**	Longer	Longer	As wide	0.5	1	ND	1.3	1	0.4	0.4	Absent	Absent	Serrated	One
A. brevis	Wider	Wider	Narrower	0.5	1	Absent	1.6	1	ND	ND	Absent	Absent	Unarmed	One
A. cilacapicus	Longer	As long as wide	As wide	0.4	1	Absent	1.7	1	0.2	0.2	Absent	Absent	Setulated	Two
***A. frutosae* n. sp.**	Longer	As long as wide	Narrower	0.6	1	ND	1.6	1	0.6	0.4	Absent	Absent	Unarmed	One
A. ghilarovi	Longer	Wider	As wide	0.6	1	Present	1	1	ND	ND	Present	Absent	Unarmed	Two
A. hadalis	Longer	Wider	Narrower	0.5	1	Absent	1.7	1	0.5	0.7	Absent	Absent	Serrated (P4)	One
A. hanseni	Longer	Wider	Narrower	0.5	1	Absent	2	1	0.8	1	Absent	Absent	Unarmed	One
*A. ingolfi**	Subequal	Wider	Narrower	0.5	1	Absent	1.7	ND	0.7	0.5	Absent	Present	Unarmed	One
***A. jani* n. sp.**	Longer	Longer	Narrower	0.6	1	Present	1.6	1	0.9	0.7	?	Absent	Distinct teeth	One
A. manganicus	Longer	Longer	Narrower	0.3	2	Absent	1.3	1	0.6	ND	Absent	Absent	Unarmed	One
A. misakiensis	Longer	Wider	Narrower	0.4	1	Absent	1.8	1	0.5	0.4	Absent	Absent	Serration	Two
***A. oharai* n. sp.**	Longer	Longer	Narrower	0.4	1	ND	1.2	1	0.8	0.8	Absent	Absent	Unarmed	One
***A. paleroi* n. sp.**	Longer	As long as wide	Narrower	0.5	1	Absent	1	1	0.7	0.7	Absent	Absent	Serrated (P5, P6)	One
***Agathotanais* sp. abyss-1**	Longer	Longer	Narrower	0.5	1	Absent	1.4	1	0.7	ND	Absent	Absent	Unarmed	One
A. spinipoda	Longer/wider	As long as wide	Narrower	0.3	1	Absent	1.4	1	ND	ND	Present	Absent	Unarmed	One
A. splendidus	Longer	As long as wide	As wide	0.3	0?	Absent	1.1	0	ND	ND	Absent?	Absent	Unarmed	One
A. toyoshioae	Longer	As long as wide	Narrower	0.3	1	Absent	1.6	1	0.4	0.4	Absent	Absent	Serrated	One

**According to Bird and Holdich (1988). Bold – new species described in the paper. ND – no data.*

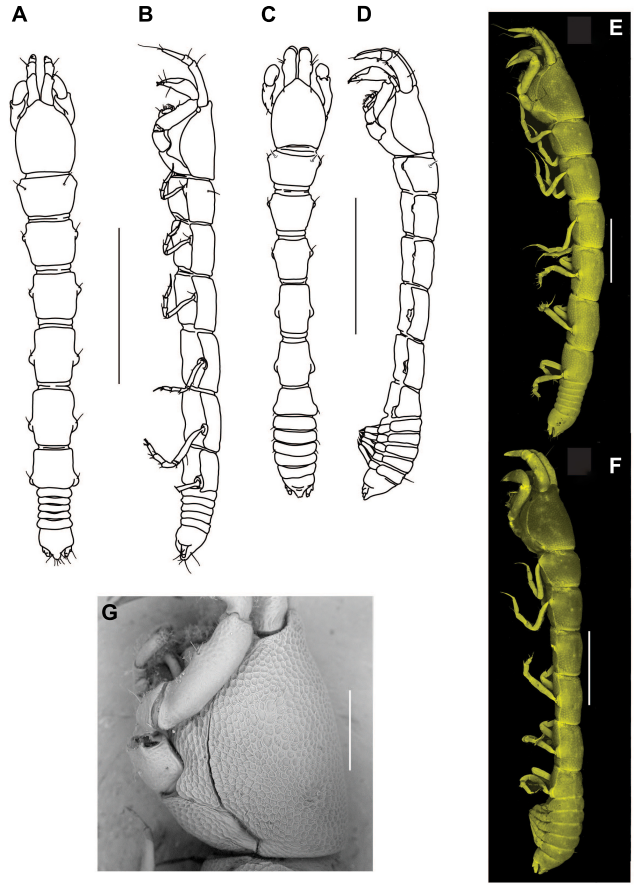

FIGURE 5 | *Agathotanais frutosae* n. sp., neuter, holotype (**A,B**: NHM 58033), juvenile male, paratype (**C,D**: ZMH K-61184), neuter, paratype (**E,G**: ZMH K-61187), juvenile male, paratype (**F**: ZMH K-61184). **(A)** dorsal view; **(B)** lateral view; **(C)** dorsal view; **(D)** lateral view; **(E)** lateral view (confocal picture); **(F)** lateral view (confocal picture); **(G)** pitted surface of body (SEM picture). Scale bars: **(A–D)** = 1 mm, **(E–F)** = 500 μm, **(G)** = 200 μm.

five neuters, 2.9–3.3 mm, SokhoBio st. 11-6, (NHM 58037); two juvenile males, 2.3–2.7 mm, three neuters, 2.9–3.1 mm, SokhoBio st. 11-6, (NHM 58038); manca II, 1.3 mm, manca III, 1.8 mm, three neuters, 2.3–3.4 mm, SokhoBio st. 11-6, (ZMH K-61187); juvenile male, 2.7 mm, SokhoBio st. 11-6, (ZMH K-61188); juvenile male, 2.3 mm, SokhoBio st. 11-6, (ZMH K-61189); neuter, 2.3 mm, SokhoBio st. 7-4, (ZMH K-61189); manca II, 1.6 mm, two mancas III, 1.6 mm, two juvenile males, 2.3–2.4 mm, five neuters, 2.3–3.2 mm, SokhoBio st. 7-4, (NHM 58039); neuter, 3.1 mm, SokhoBio st. 7-3, (NHM 58040); four mancas II, 1.3–1.7 mm, juvenile male, 2.3 mm, two neuters, 2.3–2.5 mm, SokhoBio st. 7-3, (NHM 58041); five mancas II, 1.3–1.8 mm, two mancas III, 2.1 mm, eleven neuters, 2.2–3.5 mm, SokhoBio st. 7-3, (ZMH K-61191); six mancas II, 1.3–1.5 mm, two mancas III, 1.8 mm, two juvenile males, 2.1 mm, nine neuters, 2.1–3.1 mm, SokhoBio st. 7-3, (ZMH K-61192); five juvenile males, 2.3–2.8 mm, SokhoBio st. 7-3, (ZMH K-61193); juvenile male, 2.5 mm, SokhoBio st. 2-7, (NHM 58042); juvenile male, 2.6 mm, SokhoBio st. 7-3, (NHM 58043); three juvenile males, 2.4–2.7 mm, SokhoBio st. 7-3, (NHM 58044); neuter, broken, SokhoBio st. 4-10, (NHM 58045); neuter, broken, SokhoBio st. 4-9, (ZMH K-61194); two mancas II, 1.6–1.7 mm, two juvenile males, 2.0–2.4 mm, neuter, 2.1 mm, SokhoBio st. 4-9, (ZMH K-61195); neuter, 2.9 mm, ICUL5167, SokhoBio st. 6-6, (ZMH K-61196); two juvenile males, 2.3–2.3 mm, neuter, 3.3 mm, SokhoBio st. 7-3, (ZMH K-61197); two mancas III, 1.8–1.9 mm, five neuters, 2.3–3.4 mm, SokhoBio st. 7-3, (ZMH K-61198); two neuters, 2.7–3.2 mm, SokhoBio st. 7-3, (NHM 58046); juvenile male, broken, SokhoBio st. 2–7, (NHM 58047); neuter, 3.2 mm, SokhoBio st. 3-9, (NHM 58048); juvenile male, 2.7 mm, SokhoBio st. 3-9, (NHM 58049); three mancas II, 1.4 mm, two mancas III, 1.4–1.7 mm, two juvenile males, 2.2–2.3 mm, seven neuters, 2.8–3.2 mm, SokhoBio st. 4-9, (ZMH K-61199); eight juvenile males, 2.1–3.4 mm, neuter, 3.3 mm, SokhoBio st. 2-8, (ZMH K-61200); three juvenile males, 2.6–2.7 mm, SokhoBio st. 2-7, (ZMH K-61201); three juvenile males, 2.3–2.6 mm, SokhoBio st. 2-8, (ZMH K-61202); juvenile male, 2.7 mm, SokhoBio st. 2-7, (ZMH K-61203); two mancas II, 1.4 mm, SokhoBio st. 2-7, (ZMH K-61204); three mancas III, 1.7 mm, six juvenile males, 2.1–2.6 mm, SokhoBio st. 2-7, (ZMH K-61204); fifty one neuters, 2.1–3.8 mm, SokhoBio st. 2-7, (ZMH K-61204); two juvenile males, 2.2–2.7 mm, three mancas

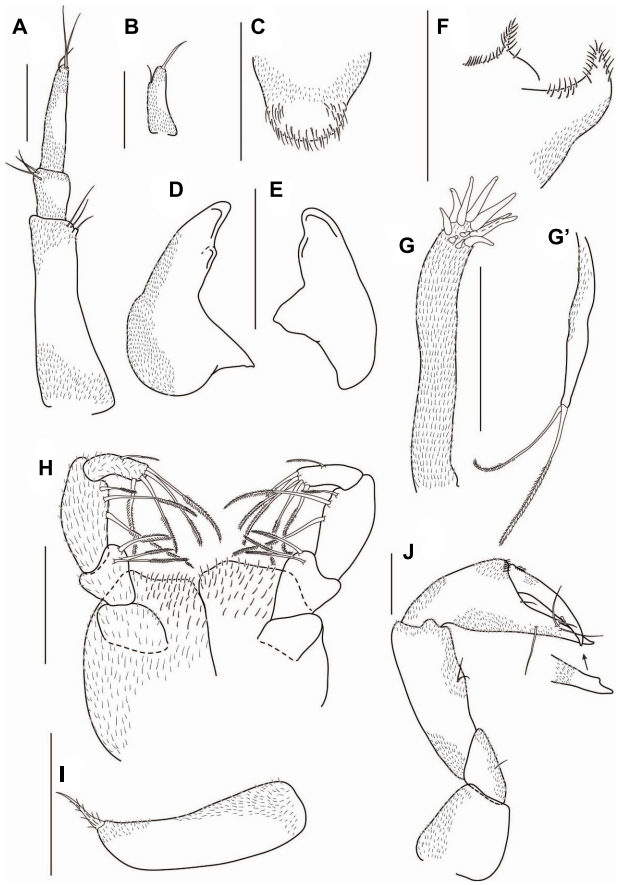

FIGURE 6 | *Agathotanais frutosae* n. sp., neuter, paratype (**A,F,J**: NHM 58034; **B–E**, **G–I**: NHM 58035). **(A)** antennule; **(B)** antenna; **(C)** labrum; **(D)** left mandible; **(E)** right mandible; **(F)** labium; **(G)** maxillule; **(G')** palp of maxillule; **(H)** maxilliped; **(I)** epignath; **(J)** cheliped. Scale bars: **(C–I)** = 10 μm, **(A,B,J)** = 100 μm.

II, 1.3–1.6 mm, SokhoBio st. 2-8, (MIMB 42497); sixteen mancas III, 1.6–2.0 mm, SokhoBio st. 2-8, (MIMB 42497); eighteen neuters, 2.2–3.7 mm, SokhoBio st. 2-8, (MIMB 42497); two mancas II, 1.3–1.4 mm, two mancas III, 1.5 mm, juvenile male, 2.4 mm, 5 neuters, 2.9–3.2 mm, SokhoBio st. 2-7, (MIMB 42498); neuter, broken, SokhoBio st. 2-7, (MIMB 42499); neuter, broken, SokhoBio st. 2-7, (MIMB 42500); four mancas III, 1.6–1.8 mm, two neuters, 2.9 mm, SokhoBio st. 2-7, (MIMB 42501); manca III, 1.9 mm, juvenile male, 3.2 mm, neuter, broken, SokhoBio st. 2-7, (MIMB 42502); six juvenile males, 2.5–3.3 mm, SokhoBio st. 2-7, (MIMB 42503); six juvenile males, 2.0–2.7 mm, SokhoBio st. 2-7, (MIMB 42504); manca II, 1.5 mm, manca III, 1.9 mm, neuter, 2.3 mm, SokhoBio st. 2-7, (MIMB 42505); manca II, 1.5 mm, SokhoBio st. 2-8, (MIMB 42506); two mancas III, 1.5–2.5 mm, two neuters, 3.0–2.4 mm, SokhoBio st. 2-7, (MIMB 42507); manca II, 1.4 mm, two mancas III, 1.6–1.8 mm, juvenile male, 2.3 mm, four neuters, 2.2–3.3 mm, SokhoBio st. 2-7, (MIMB 42508); two mancas III, 1.6–1.8 mm, five neuters, 2.2–3.3 mm, SokhoBio st. 2-8, (MIMB 42509); two juvenile males, 2.6 mm, SokhoBio st. 1-8, (MIMB 42510); two neuters, 3.2 mm, SokhoBio st. 1-9, (MIMB 42511); four neuters, 2.7–3.1 mm, SokhoBio st. 1-9, (MIMB 42512); neuter, broken, SokhoBio st. 1-8, (MIMB 42512); brooding female, 3.0 mm, 3 juvenile males, 1.8–3.3 mm, four neuters, 2.0–2.9 mm, SokhoBio st. 1-8, (MIMB 42514); juvenile male, 2.8 mm, SokhoBio st. 1-9, (MIMB 42515); juvenile male, broken, SokhoBio st. 1-9, (MIMB 42516); manca III, 1.8 mm, juvenile male, 2.3 mm, SokhoBio st. 2-7, (MIMB 42517); juvenile male, 2.3 mm, SokhoBio st. 4-9, (MIMB 42518); six juvenile males, 2.1–2.7 mm, SokhoBio st. 4-10, (MIMB 42519); manca, broken, SokhoBio st. 4-9, (MIMB 42520); juvenile male, 2.9 mm, neuter, 3.0 mm, SokhoBio st. 4-9, (MIMB 42521); juvenile male, 2.2 mm, SokhoBio st. 4-9, (MIMB 42522); juvenile male, 2.5 mm, SokhoBio st. 4-9, (MIMB 42523); juvenile male, 2.7 mm, SokhoBio st. 4-9, (MIMB 42524); five juvenile males, 2.3–2.7 mm, SokhoBio st. 4-10, (MIMB 42525); manca, broken, SokhoBio st. 11-6, (MIMB 42527); eight mancas II, 1.4–1.7 mm, two mancas III, 1.7–1.8 mm, four neuters, 2.2–3.5 mm, SokhoBio st. 11-6, (MIMB 42526).

Diagnosis of neuter: Body narrow (7.7 L:W). Carapace without pair of lateral setae in posterior margin. Pereonite-1 with pair of dorsal setae. Pereonites 4–6 longer than wide. Pereonite-6 0.9× pleonites 1–5 combined. Pleonites 1–5 narrower than pereonite-6. Antennule article-1 longer than other articles combined, about 1.6× article-3. Antenna one-articled. Cheliped palm 1.6 L:W. Pereopods 2–3 carpus with dorsodistal seta, 0.6× and 0.4× propodus, respectively. Pereopods 4–6 unguis unarmed. Uropod endopod one-articled.

Etymology: Species is dedicated to Dr. Inmaculada Frutos (University of Łódź), our colleague and peracarid specialist, who collected tanaids during the SokhoBio expedition to the Sea of Okhotsk.

Description of neuter: Body from the holotype (NHM 58033), appendages from paratypes (NHM 58034 and 58035). BL = 3.0 mm. Body (**Figures 5A,B,E,G**) 7.7 L:W, cylindrical. Carapace 1.1 L:W, 0.1× BL. Pereon 0.6× BL. Pereonites 1–6: 0.7, 0.8, 1.0, 1.3, 1.3, and 0.8 L:W, respectively. Pereonite-1 with pair of setae in the proximal half of the dorsal surface. Pleon with pleotelson 0.1× BL. Pleonites 1–5 0.4 L:W each. Pleotelson dorsally 0.7× pleonites 1–5.

Antennule (**Figure 6A**) article-1 3.5 L:W, 3.7× article-2, with three distal setae; article-2 1.2 L:W, 0.4× article-3, with three distal setae; article-3 4.5 L:W, with two distal and one subdistal setae.

Antenna (**Figure 6B**) one-articled, 2.8 L:W, with one subdistal and one distal seta.

Mouthparts: Labrum (**Figure 6C**) hood-shaped, covered by numerous setae of different lengths.

Left mandible (**Figure 6D**) incisor with a blunt tooth, *lacinia mobilis* short and rounded.

Right mandible (**Figure 6E**) incisor with rounded tooth.

Labium (**Figure 6F**) with the spiniform distal process and lateral process, covered by numerous setae.

Maxillule endite (**Figure 6G**) with eleven distal spines. Palp (**Figure 6G'**) with two plumose terminal setae.

Maxilliped (**Figure 6H**) palp article-1 rectangular, naked; article-2 0.8 L:W, with three inner plumose setae; article-3 2.2 L:W, with three inner plumose setae; left palp article-4 with

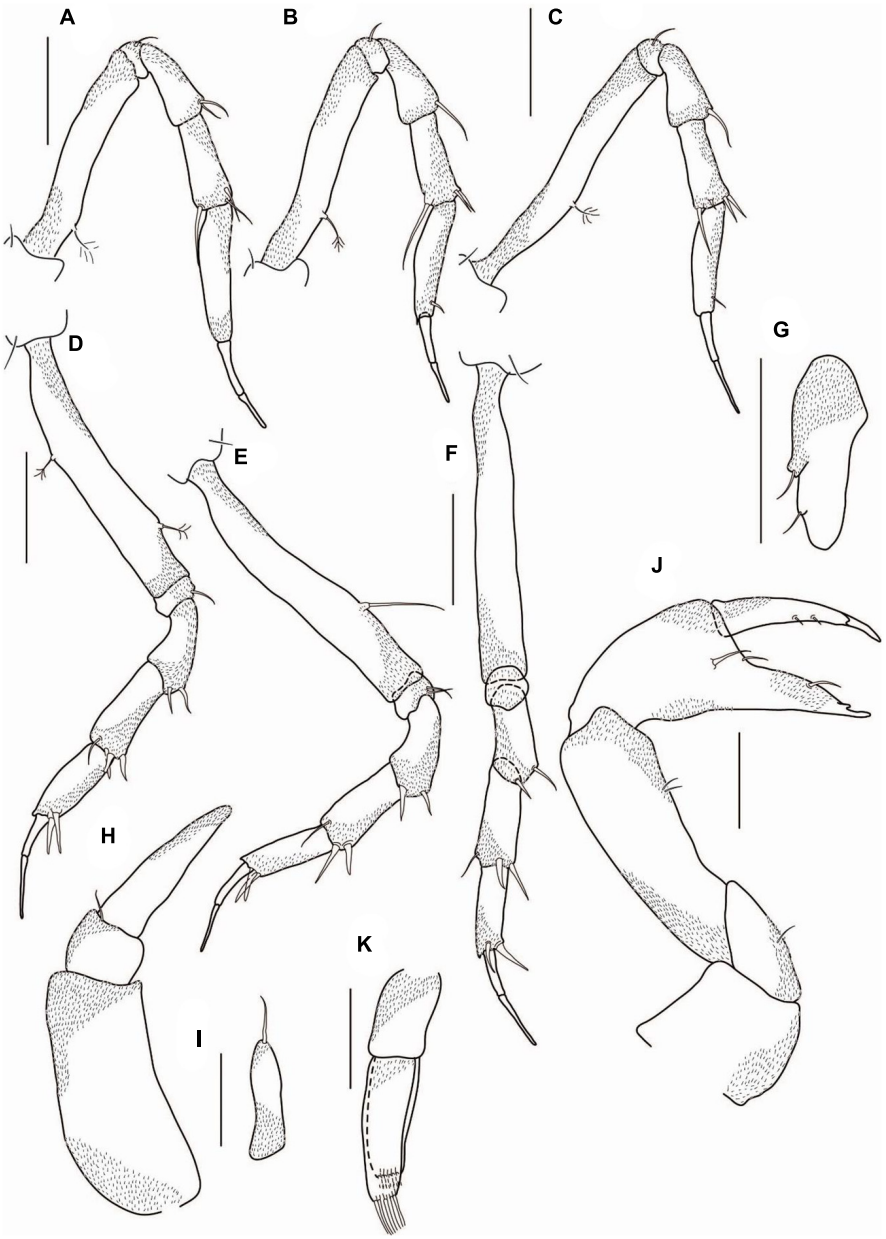

FIGURE 7 | *Agathotanais frutosae* n. sp., neuter, paratypes (**A–G**: NHM 58034); juvenile male, paratype (**H–K**: ZMH K-61184). **(A)** peropod-1; **(B)** pereopod-2; **(C)** pereopod-3; **(D)** pereopod-4; **(E)** pereopod-5; **(F)** pereopod-6; **(G)** uropod; **(H)** antennule; **(I)** antenna; **(J)** cheliped; **(K)** pleopod. Scale bar: **(A–K)** = 100 μm.

four plumose distal and plumose outer setae; right palp article-4 with five plumose distal setae and with plumose outer seta. Basis covered with dense, numerous setae of different lengths.

Epignath (**Figure 6I**) elongated, with plumose, robust terminal seta.

Cheliped (**Figure 6J**) basis 1.0 L:W, naked; merus with midventral seta; carpus 2.5 L:W, slightly shorter than propodus and fixed finger combined, with two midventral setae; palm 1.6 L:W, with a row of short setae near dactylus insertion; fixed finger 0.6× palm, cutting edge with distal protrusion and three setae, one ventral seta, distal spine small; dactylus 1.1× fixed finger, cutting edge with midlength spine; unguis sharp.

Pereopod-1 (**Figure 7A**) coxa with seta; basis 6.2 L:W, 2.4× merus, with penicillate dorsoproximal seta; ischium with ventrodistal seta; merus 2.5 L:W and 0.9× carpus, with two ventrodistal setae; carpus 2.5 L:W, 0.6× propodus, with two ventrodistal setae, and with long (0.4× propodus) dorsodistal seta; propodus 4.6 L:W, 1.3× dactylus and unguis combined, naked; dactylus 1.4× unguis, unarmed; unguis unarmed, with rounded tip.

Pereopod-2 (**Figure 7B**) coxa with seta; basis 6.0 L:W, 2.8× merus, with penicillate, dorsoproximal seta; ischium with ventrodistal seta; merus 2.3 L:W, 0.8× carpus, with ventrodistal seta; carpus 2.7 L:W, 0.7× propodus, with two short ventrodistal setae, and long (0.6× propodus) dorsodistal seta; propodus 4.0 L:W, with ventrosubdistal short seta, and with spinules near dactylus insertion; dactylus 0.8× unguis, unarmed; unguis unarmed, with rounded tip.

Pereopod-3 (**Figure 7C**) coxa with seta; basis 8.0 L:W, 3.6× merus, with penicillate dorsoproximal seta; ischium with ventrodistal seta; merus 2.0 L:W, 0.8× carpus, with ventrodistal seta; carpus 2.7 L:W, 0.8× propodus, with two ventrodistal, one short middistal, and one long (0.4× propodus) dorsodistal setae; propodus 3.7 L:W, 1.0× dactylus and unguis combined, with ventrosubdistal seta; dactylus 0.8× unguis, unarmed; unguis unarmed, with rounded tip.

Pereopod-4 (**Figure 7D**) coxa with seta; basis 6.3 L:W, 3.3× merus, with two penicillate setae: one dorsal and one ventral; ischium with ventrodistal seta; merus 2.0 L:W, 0.8× carpus, with two ventrodistal setae; carpus 2.3 L:W, 1.0× propodus, with three robust ventrodistal and one simple dorsodistal setae; propodus 2.4 L:W, 0.8× dactylus and unguis combined, with two robust ventrodistal setae; dactylus 0.7× unguis, unarmed; unguis unarmed, with rounded tip.

Pereopod-5 (**Figure 7E**) coxa with seta; basis 7.0 L:W, 3.0× merus, with middorsal seta; ischium with two ventrodistal setae; merus 2.4 L:W, 1.0× carpus, with two robust ventrodistal setae; carpus 2.2 L:W, 1.0× propodus, with two robust ventrodistal setae and simple dorsodistal seta; propodus 3.0 L:W, with two strong ventrodistal setae; dactylus 0.7× unguis, unarmed; unguis unarmed, with rounded tip.

Pereopod-6 (**Figure 7F**) coxa with seta; basis 7.2 L:W, 3.0× merus; ischium naked; merus 2.5 L:W, 0.9× carpus, with two ventrodistal setae; carpus 2.7 L:W, 1.2× propodus, with two robust ventrodistal and simple dorsodistal setae; propodus 3.4 L:W, 0.8× dactylus and unguis combined, with two robust (ventrodistal and middistal) setae; dactylus 0.7× unguis, unarmed; unguis unarmed, with rounded tip.

Pleopods absent.

Uropod (**Figure 7G**) exopod reduced and fused with basal article, tipped with seta; endopod one-articled, 3.0 L:W, with lateral seta.

Description of juvenile male: Body from paratype (ZMH K-61184), appendages from paratype (ZMH K-61183). BL = 3.0 mm. Body 7.6 L:W (**Figures 5C,D,F**). Carapace 1.1 L:W, 0.1× BL. Pereon 0.6× BL, pereonites 1–6: 0.5, 0.8, 1.0, 1.5, 1.3, and 0.6 L:W, respectively. Pleon combined with pleotelson 0.2× BL. Pleonites 1–5 0.3 L:W each. Pleotelson directed backward.

Antennule (**Figure 7H**) article-1 2.4 L:W, 1.4× article-3, naked; article-2 0.8 L:W, 0.3× article-3, with distal seta; article-3 2.5 L:W, naked.

Antenna (**Figure 7I**) one-articled, 3.7 L:W, tipped with seta.

Cheliped (**Figure 7J**) basis 0.9 L:W; merus with midventral seta; carpus 3.0 L:W, 1.7× palm; palm 1.3 L:W, with two setae near dactylus insertion; fixed finger 3.4 L:W, 1.0× palm, cutting edge with a proximal protrusion, with seta and small distal spine; dactylus 6.0 L:W, cutting edge with two spines on inner margin, unguis slender.

Pleopods (**Figure 7K**) endopod with eight setae along distal margin; exopod 0.8× endopod, with eight setae along the distal margin.

Intraspecific variation: Manca II: length 1.3–1.8 mm.

Manca III: length 1.5–2.1 mm.

Neuter: length 2.0–3.8 mm; maxilliped palp article-4 with four/five distal seta on left and right palp, respectively; cheliped carpus with one/two midventral seta; pereopod-5 ischium with one/two ventrodistal setae; pereopod-6 ischium with zero/one ventrodistal seta.

Juvenile male: length 1.8–3.4 mm; antenna article-2 with zero/two distal setae; article-3 with one/three simple setae distally; cheliped fixed finger with one/three ventral setae.

Distribution: NW Pacific, Sea of Okhotsk, Kuril Basin (**Figure 2**); depth range: 3206–3374 m.

Remarks. A pair of dorsal setae on pereonite-1 is a unique feature of *A. frutosae* n. sp. Moreover *A. frutosae* belongs to the species of *Agathotanais* with an elongated cheliped palm (L:W >1.6), together with *A. ahyongi*, *A. cilacapicus*, *A. brevis*, *A. hadalis*, *A. hanseni*, *A. ingolfi*, *A. misakiensis*, *A. toyoshioae,* and *A. jani.* All the other species have a chelipedal palm clearly shorter (*A. ghilarovi*, *A. splendidus,* and *A. oharai*, is 1.0–1.2 L:W), or slightly shorter (*A. beatae, A. manganicus*, *A. spinipoda,* and *Agathotanais* sp. abyss-1 it is 1.3–1.4 L:W) (**Table 1**).

From the *Agathotanais* with elongated palm, *A. frutosae* can be distinguished by unarmed dactylus and unguis of pereopods 4–6. Unguis is serrated in *A. hadalis*, *A. misakiensis*, and *A. toyoshioae*; *A. cilacapicus* has a setulose unguis; *A. jani* has distinct teeth on unguis, and *A. ingolfi* has a small accessory spine on its dactylus, near the unguis. An unarmed dactylus and unguis are also present in *A. hanseni*, *A. ahyongi* and *A. brevis*. However, *A. frutosae* differs from *A. hanseni* and *A. ahyongi* in the length of the dorsodistal carpal seta of pereopods 2 and 3. It is 0.6 in relation to propodus in *A. frutosae,* and 0.8 and 1.0 in *A. hanseni*; *A. ahyongi* has only two short carpal setae in pereopods 2 and 3 (about 0.1 of propodus length) (**Table 1**).

Agathotanais jani n. sp. Jóźwiak and Pełczyńska.

This species is register under the zoobank number: LSIDurn:lsid:zoobank.org:act:375FCFD9-C32B-4248-9F52-583A6037179F

(**Figures 8–10**)

Material examined: Holotype: neuter, 3.8 mm, JPIO SO239 st. 118, (ZMH-K-61149).

Paratype: neuter, dissected on slides, JPIO st. 99, (ZMH-K-61150); neuter, 2.5 mm, JPIO st. 99, (ZMH-K-61151); juvenile male damaged, JPIO st. 99, (ZMH-K-61152); specimen damaged, JPIO st. 81, (ZMH-K-61153); specimen damaged, JPIO st. 81, (ZMH-K-61154); juvenile male, 2.4 mm, JPIO st. 118, (ZMH-K-61155); neuter, 2.8 mm, JPIO st. 59, (ZMH-K-61156); neuter, broken, JPIO st. 59, (ZMH-K-61157); neuter, damaged, JPIO st.

24, (ZMH-K-61158); juvenile male, damaged, JPIO st. 24, (ZMH-K-61159); neuter, broken, JPIO st. 50, (ZMH-K-61160); juvenile male, broken, JPIO st. 99, (ZMH-K-61161); neuter, 2.9 mm, JPIO st. 20, (ZMH-K-61162); neuter, damaged, JPIO st. 20, (ZMH-K-61163); juvenile male, 3.0 mm, JPIO st. 57, (ZMH-K-61164); juvenile male, 3.2 mm, JPIO st. 57, (ZMH-K-61165); juvenile male, broken, JPIOst. 12, (ZMH-K-61166); specimen damaged, JPIO st. 12, (ZMH-K-61167); neuter, 2.9 mm, JPIO st.12, (ZMH-K-61168); neuter, broken, JPIO st. 12, (ZMH-K-61169).

Diagnosis of neuter: Body narrow (about 12.8 L:W). Carapace without pair of lateral setae in posterior margin. Pereonite-1 without pair of dorsal setae. Pereonites 4–6 longer than wide. Pereonite-6 as long as pleonites 1–5 combined. Pleonites 1–5 as wide as pereonite-6. Antennule article-1 longer than remaining articles combined, less than 2.0× article-3. Antenna one-articled. Cheliped palm 1.6 L:W. Pereopods 2–3 carpus with dorsodistal seta 0.9× and 0.7× propodus, respectively. Pereopods 4–6 unguis with distinct, pointed ventral teeth – two in pereopod-4 and three in pereopods 5–6. Uropod endopod one-articled.

Etymology: The species is dedicated to Jan Jóźwiak, beloved son of PJ.

Description of neuter: Body from the holotype (ZMH-K-61149), appendages from paratype (ZMH-K-61150). BL = 3.6 mm. Body (**Figures 8A,B**) 12.8 L:W, elongated. Carapace 1.3 L:W, 0.2× BL. Pereon 0.8× BL. Pereonites 1–6: 0.6, 1.1, 1.4, 1.5, 1.9, and 1.2 L:W, respectively. Pleon with pleotelson 0.1× BL. Pleonites 1–5 0.3 L:W each. Pleotelson in dorsal view 0.7× pleonites 1–5, almost square, apex pointed, directed backward.

Antennule (**Figure 9A**) article-1 4.9 L:W, 4.3× article-2, with three subdistal setae; article-2 1.5 L:W, 0.4× article-3, with outer subdistal seta; article-3 4.6 L:W, with seven distal setae.

Antenna (**Figure 9A**) one-articled, 2.5 L:W, with long distal seta (one distal seta broken).

Mouthparts: Labrum (**Figure 9B**) hood-shaped, covered with numerous setae of different lengths.

Left mandible (**Figure 9C**) incisor with three small rounded teeth; *lacinia mobilis* rounded and short.

Right mandible (**Figure 9D**) incisor with three rounded teeth.

Maxillule endite (**Figures 9E,E'**) with eleven robust distal spines of various lengths and numerous setules along outer and inner margin; palp not observed.

Maxilla (**Figure 9F**) elongated and simple.

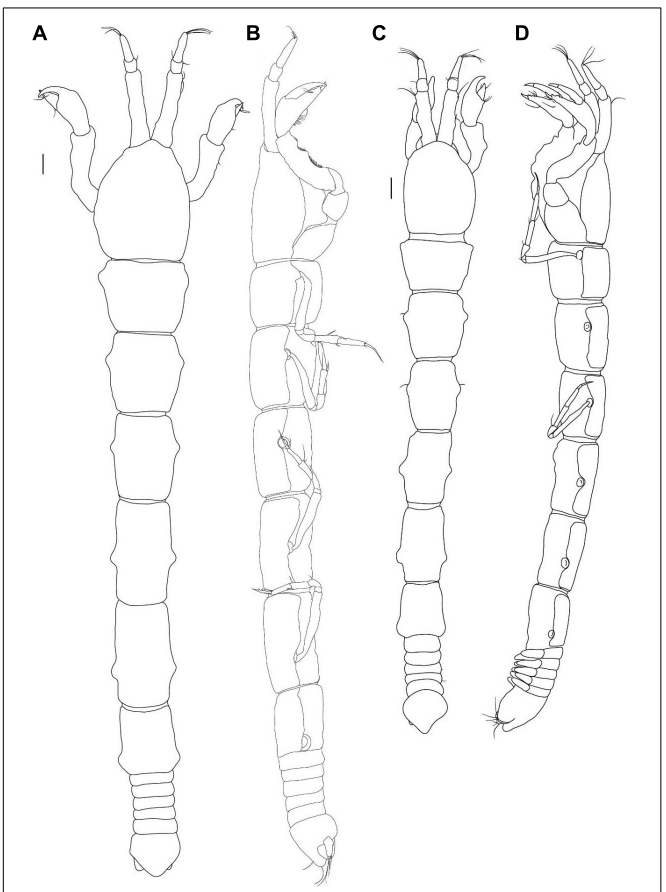

FIGURE 8 | *Agathotanais jani* n. sp., neuter, holotype (**A,B**: ZMH-K-61149), juvenile male, paratype (**C,D**: ZMH-K-61159). **(A)** Dorsal view; **(B)** lateral view; **(C)** dorsal view; **(D)** lateral view. Scale bar: **(A–D)** = 100 μm.

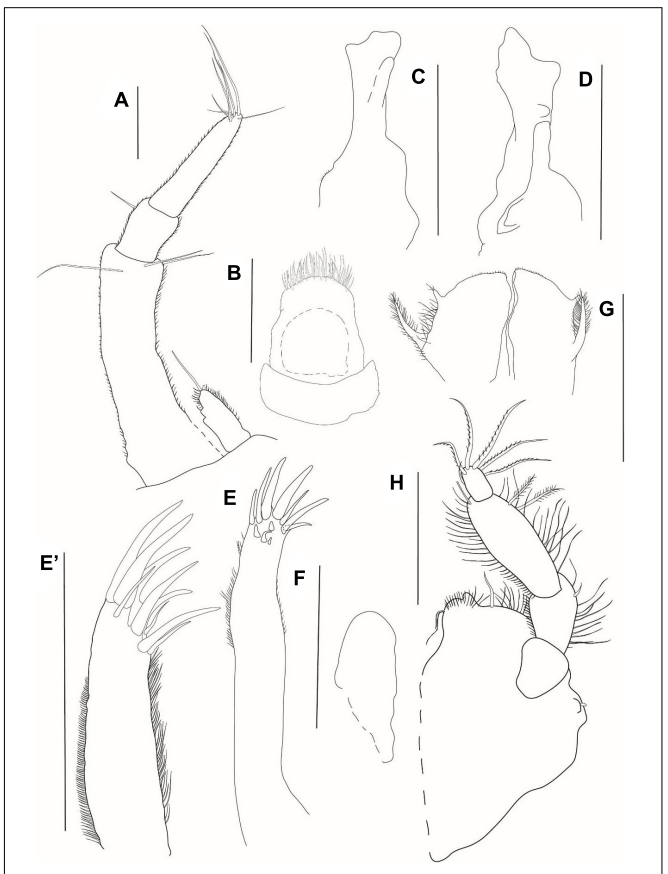

FIGURE 9 | *Agathotanais jani* n. sp., neuter, paratype (ZMH-K-61150). **(A)** antennule and antenna; **(B)** labrum; **(C)** left mandible; **(D)** right mandible; **(E)** maxillule; **(E')** details of maxillule; **(F)** maxilla; **(G)** labium; **(H)** maxilliped. Scale bar: **(A–H)** = 10 μm.

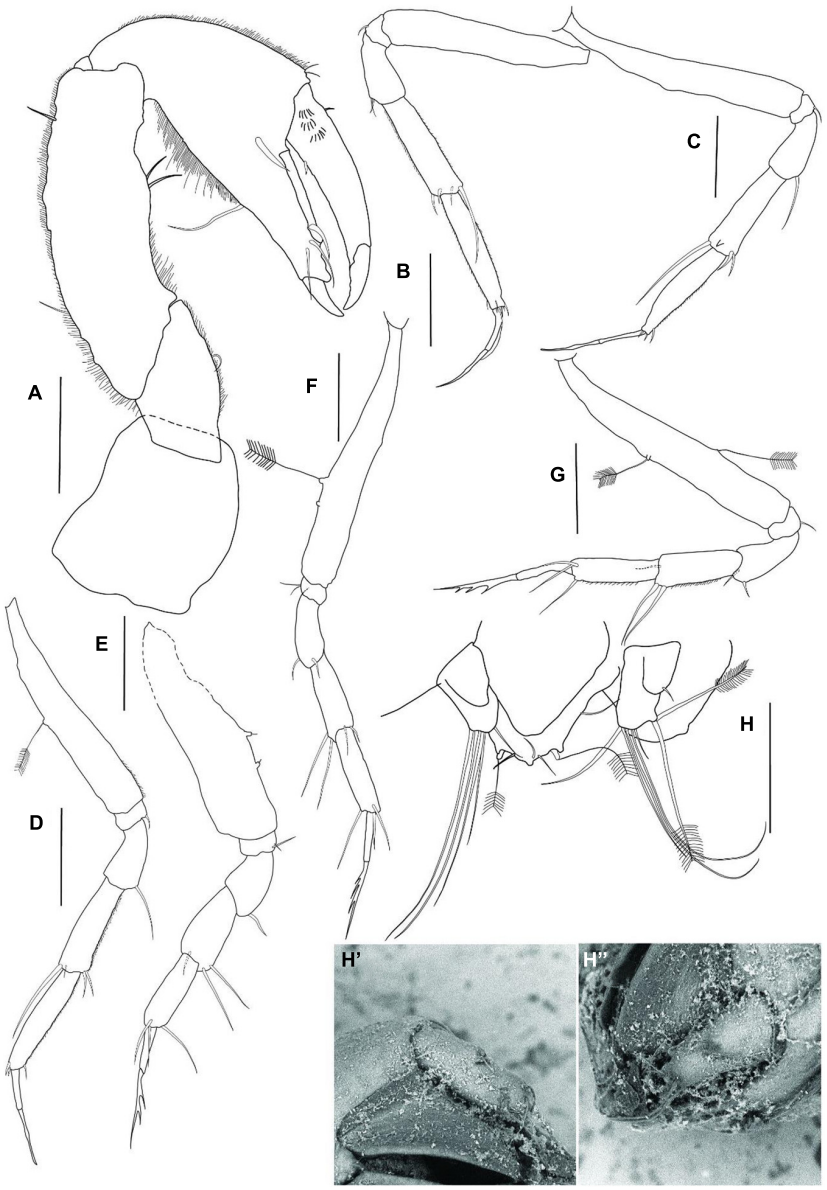

FIGURE 10 | *Agathotanais jani* n. sp., neuter, paratype (ZMH-K-61150). **(A)** cheliped; **(B)** pereopod-1; **(C)** pereopod-2; **(D)** pereopod-3; **(E)** pereopod-4; **(F)** pereopod-5; **(G)** pereopod-6; **(H)** uropod; **(H')** detail of uropod – ventral view (SEM picture); **(H")** detail of uropod – lateral view (SEM picture). Scale bar: **(A–D)** = 100 μm.

Labium (**Figure 9G**) with the spiniform distal process and long lateral process, covered by numerous setae.

Maxilliped (**Figure 9H**) endite with gustatory cups seta and numerous fine setae on distal margin; palp article-1 1.3 L:W, naked; article-2 1.4 L:W, with inner seta and numerous fine setae of various lengths on inner and outer margins; article-3 2.4 L:W, with two inner subdistal plumose setae, margins with numerous fine setae; article-4 1.7 L:W, with one subdistal and five serrated distal setae. Endites short with one midlength seta and numerous fine setae distally.

Cheliped (**Figure 10A**) basis 0.9 L:W, naked; merus with midventral seta; carpus 3.0 L:W, marginally shorter than propodal palm and fixed finger combined, with two midventral setae and two dorsal (one proximal and one subdistal) setae; palm 2.5 L:W, with robust seta at dactylus insertion; fixed finger subequal to palm, with long ventral seta, cutting edge gently undulated with three setae, distal spine robust; dactylus as long as a fixed finger, with dorsoproximal short seta, cutting edge with proximal seta; unguis robust.

Pereopod-1 (**Figure 10B**) basis 6.2 L:W, naked; ischium with ventrodistal seta; merus 2.0 L:W, 0.5× carpus, with two ventrodistal setae; carpus 3.6 L:W, 0.9× propodus, with three short distal setae and long (0.6× propodus) dorsodistal seta;

propodus 5.5 L:W, 2.7× dactylus and unguis combined, with short ventrodistal seta and some spinules near dactylus insertion; dactylus 8.0 L:W, 0.7× unguis, with proximal seta; unguis unarmed, with a pointed tip.

Pereopod-2 (**Figure 10C**) basis 8.1 L:W, naked; ischium with ventrodistal seta; merus 2.1 L:W, 0.7× carpus, with long ventrodistal seta; carpus 3.5 L:W, 0.9× propodus, with two ventrodistal setae, and long (0.9× propodus) dorsodistal seta; propodus 4.6 L:W and 2.5× dactylus and unguis combined, distally damaged, with short ventrodistal seta and some spinules near dactylus insertion; dactylus 13.0 L:W, 1.0× unguis, unarmed; unguis unarmed, with a pointed tip.

Pereopod-3 (**Figure 10D**) basis 6.8 L:W, with penicillate dorsal seta; ischium with ventrodistal seta; merus 2.0 L:W, 0.7× carpus, with long ventrodistal seta; carpus 3.4 L:W, 0.8× propodus, with two ventrodistal setae, short and long (0.7× propodus) dorsodistal setae; propodus 5.1 L:W and 2.8× dactylus and unguis combined, with short ventrodistal seta and spinules near dactylus insertion; dactylus 6.7 L:W, 0.7× unguis, unarmed; unguis unarmed, with a pointed tip.

Pereopod-4 (**Figure 10E**) basis partly broken, with two penicillate ventral setae; ischium with two ventrodistal setae; merus 1.3 L:W, 0.7× carpus, with ventrodistal seta; carpus 1.9 L:W, 0.9× propodus, with two long ventrodistal and one dorsodistal setae; propodus 3.0 L:W, with two dorsodistal and ventrodistal setae; dactylus 5.7 L:W, 0.5× unguis; unguis with two pointed ventral teeth.

Pereopod-5 (**Figure 10F**) basis 7.4 L:W, with two penicillate midventral setae; ischium with two short ventrodistal setae; merus 2.6 L:W, 0.9× carpus, with two short ventrodistal setae; carpus 2.9 L:W, 0.8× propodus, with two long ventrodistal and two short dorsodistal setae; propodus 4.1 L:W and 2.7× dactylus and unguis combined, with two dorsodistal and one ventrodistal setae; dactylus 4.5 L:W, 0.4× unguis; unguis with three pointed ventral teeth.

Pereopod-6 (**Figure 10G**) basis 7.4 L:W, with one middorsal and one midventral penicillate setae; ischium with ventrodistal seta; merus 1.6 L:W, 0.6× carpus, with two ventrodistal setae; carpus 2.7 L:W, 1.0× propodus, with two long ventrodistal and one distal setae; propodus 3.8 L:W and 1.5× dactylus and unguis combined, with ventrodistal seta and two dorsodistal setae; dactylus 7.5 L:W, 0.7× unguis; unguis with three pointed ventral teeth.

Pleopods absent.

Left uropod (**Figures 10H,H',H"**) exopod reduced and fused with basal article, tipped with seta; endopod one-articled, with four distal and two plumose subdistal setae.

Description of juvenile male: Body and appendages from paratype (ZMH-K-61159). BL = 2.8 mm. Body (**Figures 8C,D**) elongated, 13.1 L:W; carapace 1.8 L:W. Pereonites 1–6: 0.8, 1.2, 1.5, 1.7, 1.7, and 1.2 L:W, respectively. Pleon combined with pleotelson 0.1× total body length. Pleonites 1–5 equal, 0.2 L:W each. Pleotelson 0.8× pleonites 1–6 combined, almost square in the dorsal view, apex pointed, directed backward. Appendages similar to those observed in neuters, but in juvenile males, pleopods are present although not fully developed.

Intraspecific variation: Manca III: length 1.3–1.8 mm.

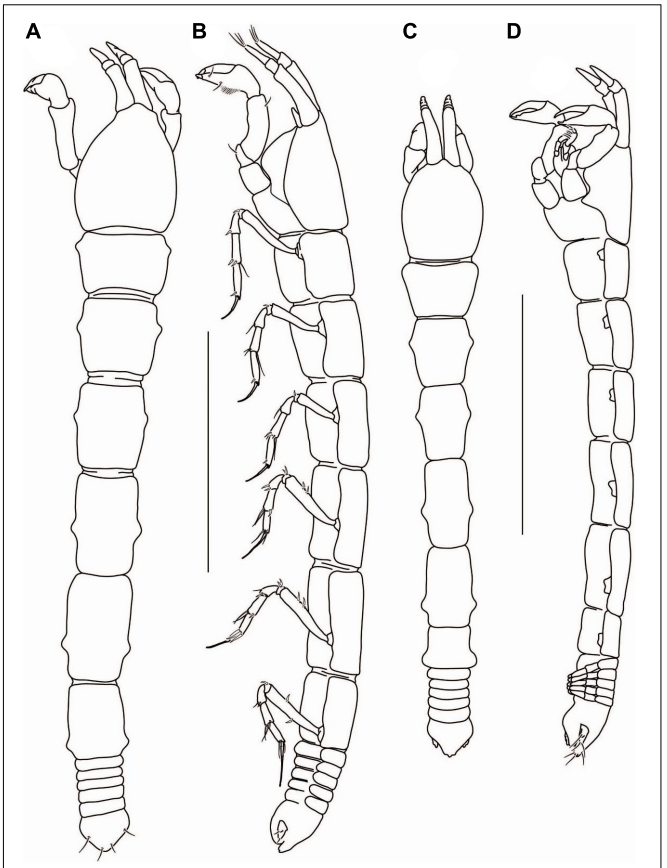

FIGURE 11 | *Agathotanais oharai* n. sp., neuter, holotype (**A,B**: NMV J 74742), juvenile male, paratype (**C,D**: NMV J 74725). **(A)** dorsal view; **(B)** lateral view; **(C)** dorsal view; **(D)** lateral view. Scale bar: **(A–D)** = 1 mm.

Neuter: length: 2.5–3.8 mm; uropod endopod with zero/two plumose setae distally (might be differences between right and left uropod).

Juvenile male: length 2.4–3. 2 mm.

Distribution: Central Pacific, Clarion-Clipperton Fracture Zone (IOM, BGR, GSR, APEI-3) (**Figure 2**); depth range: 4093–4511 m.

Remarks. The presence of distinct pointed ventral teeth on the unguis in pereopods 4–6 is a unique character that allows distinguishing *A. jani* from congeners. In *A. hadalis*, *A. misakiensis*, *A. toyoshioae, A. paleroi,* and *A. beatae* only a weak serration is present (Larsen, 2007; Kakui and Kohtsuka, 2015), while in other *Agathotanais* species the unguis in those pereopods is unarmed (**Table 1**).

***Agathotanais oharai* n. sp. Stępień, Jakiel and Błażewicz.**

This species is register under the zoobank number: LSIDurn:lsid:zoobank.org:act:C3E44847-F819-4CCE-A2AF-687C060321D9

(**Figures 11–13**)

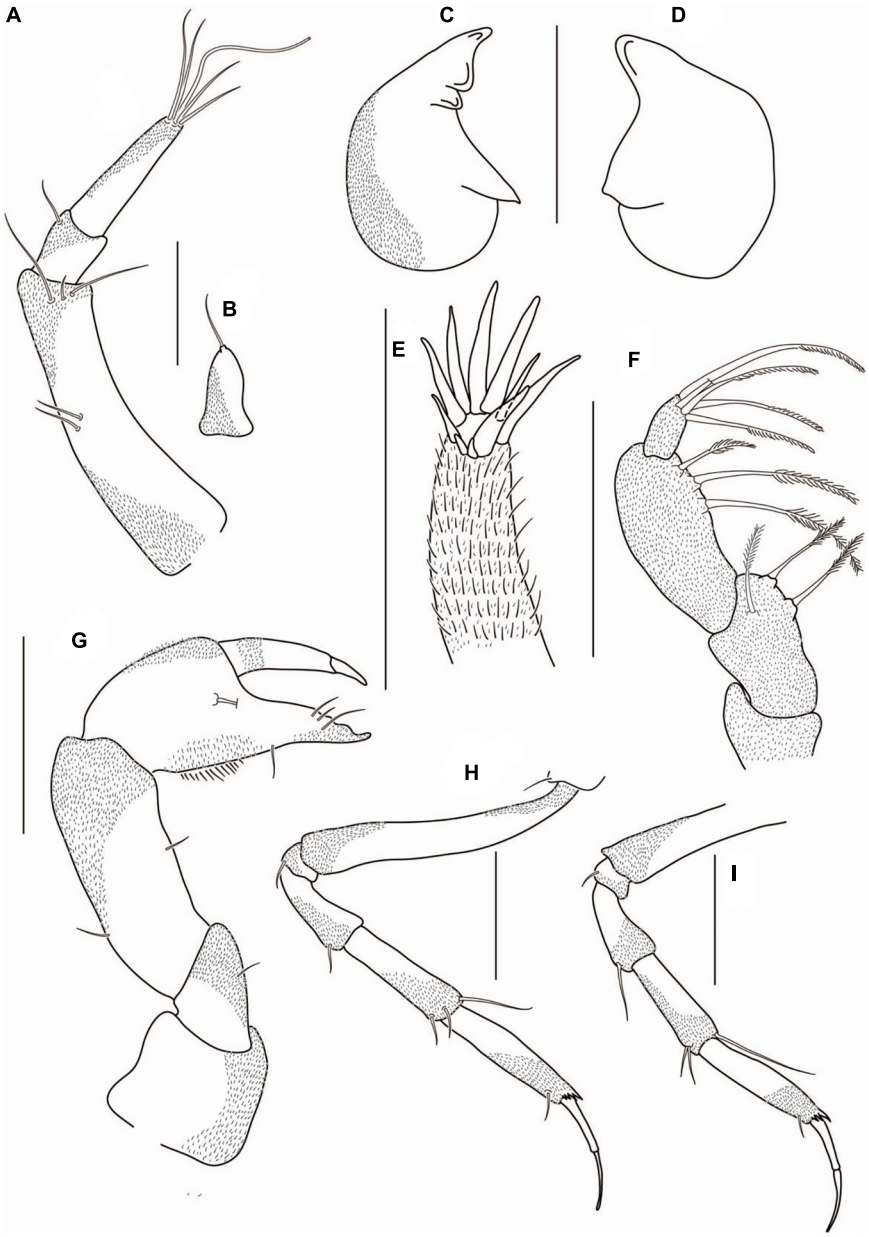

FIGURE 12 | *Agathotanais oharai* n. sp., neuter, paratype (NMV J 74742); **(A)** antennule; **(B)** antenna; **(C)** left mandible; **(D)** right mandible; **(E)** maxillule; **(F)** maxilliped; **(G)** cheliped; **(H)** pereopod-1; **(I)** pereopod-2. Scale bars: **(A–F)** = 10 μm, **(G–I)** = 100 μm.

Material examined: Holotype: neuter, 3 mm, ABYSS st. 42, (NMV J 74742).

Paratype: juvenile male, 2.5 mm, partly dissected on slides, ABYSS st. 33, (NMV J 74725); neuter, broken, dissected on slides ABYSS st. 42, (NMV J 74742).

Diagnosis of neuter: Body narrow (about 7.3 L:W). Carapace without pair of lateral setae on posterior margin. Pereonite-1 without pair of dorsal setae. Pereonites 4–6 longer than wide. Pereonite-6 1.3× pleonites 1–5 combined. Pleonites 1–5 little narrower than pereonite-6. Antennule article-1 longer than the remaining articles combined, about 2.0× article-3. Antenna one-articled. Cheliped palm 1.1 L:W. Pereopods 2–3 carpus with dorsodistal seta 0.8× propodus. Pereopods 4–6 unguis unarmed. Uropod endopod one-articled.

Etymology: The species is named in honor of Tim O'Hara, senior curator of the Marine Invertebrates Section in Museums Victoria (Melbourne) and specialist in biogeography.

Description of neuter: Body from the holotype (NMV J 74742), appendages from paratype (NMV J 74725). BL = 3 mm. Body (**Figures 11A,B**) 7.3 L:W. Carapace 1.0 L:W, 0.2× BL. Pereon 0.7× BL, pereonites 1–6: 0.6, 0.9, 1.2, 1.4, 1.7, and 1.3 L:W, respectively, rectangular in dorsal view. Pleon with

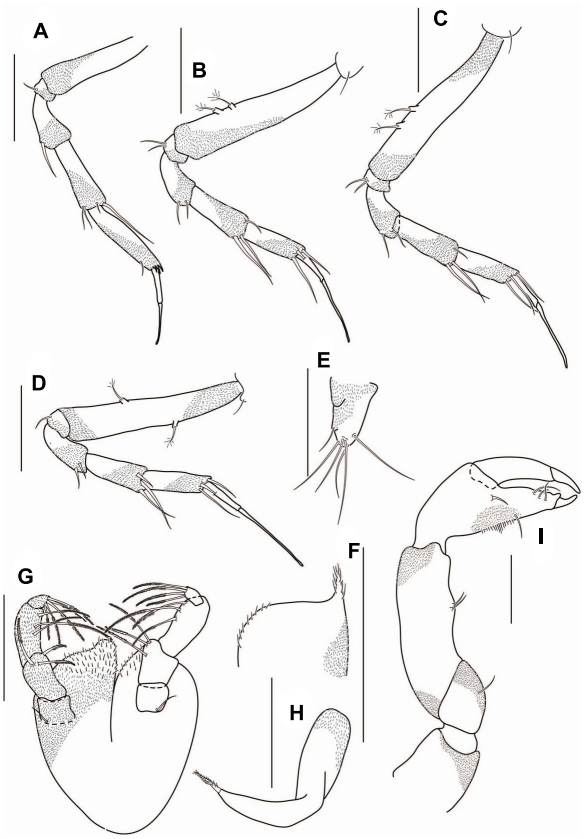

FIGURE 13 | *Agathotanais oharai* n. sp., neuter, paratype (**A–E**: NMV J 74742), juvenile male (**F–I**: NMV J 74725). **(A)** pereopod-3; **(B)** pereopod-4; **(C)** pereopod-5; **(D)** pereopod-6; **(E)** uropod; **(F)** labium; **(G)** maxilliped; **(H)** epignath; **(I)** cheliped. Scale bars: **(A–E,I)** = 100 μm; **(F–H)** = 10 μm.

pleotelson 0.1× BL. Pleonites 1–6 0.1 L:W each. Pleotelson in dorsal view 1.3× pleonites 5–6, with two pairs of lateral setae.

Antennule (**Figure 12A**) article-1 4.5 L:W, 4.3× article-2, with two midlength setae, and with three subdistal setae; article-2 1.7 L:W, 0.5× article-3, with outer distal seta; article-3 3.7 L:W, with four setae and aesthetasc distally.

Antenna (**Figure 12B**) one-articled, 1.8 L:W, tipped with seta.

Mouthparts: Left mandible (**Figure 12C**) incisor with two blunt teeth, *lacinia mobilis* short and rounded.

Right mandible (**Figure 12D**) incisor with a broad triangular tooth.

Maxillule endite (**Figure 12E**) with ten distal spines.

Maxiliped (**Figure 12F**) palp article-1 broken, naked distally; article-2 1.8 L:W, with three inner plumose setae; article-3 2.2 L:W, with three inner plumose setae; article-4 left palp 1.3 L:W, with five inner plumose distal setae.

Cheliped (**Figure 12G**) basis 0.8 L:W, with small subventral seta; merus with midventral seta; carpus 2.5 L:W, marginally shorter than propodus and fixed finger combined, with one middorsal and one midventral setae; palm 1.2 L:W, with seta near dactylus insertion and a row of ventral setae; fixed finger 0.8× palm, with one ventral seta, cutting edge with three tubercles and three setae, terminal spine small; dactylus as long as a fixed finger, curved, naked; unguis moderate size.

Pereopod-1 (**Figure 12H**) coxa with seta; basis 7.0 L:W, 3.0× merus, naked; ischium with ventrodistal seta; merus 2.0 L:W and 0.7× carpus, with ventrodistal seta; carpus 3.2 L:W, 0.9× propodus, with two ventrodistal setae and long (0.5× propodus) dorsodistal seta; propodus 3.8 L:W, 1.0× dactylus and unguis combined, with projections near dactylus insertion and ventrosubdistal seta; dactylus 1.1× unguis, unarmed; unguis unarmed, with rounded tip.

Pereopod-2 (**Figure 12I**) basis broken; ischium with ventrodistal seta; merus 1.8 L:W, 0.7× carpus, with ventrodistal seta; carpus 2.7 L:W, 0.8× propodus, with two short ventrodistal and one long (0.8× propodus) dorsodistal setae; propodus 4.7 L:W, 1.0× dactylus and unguis combined, with spinules near dactylus insertion and ventrosubdistal seta; dactylus 0.7× unguis, unarmed; unguis unarmed, with rounded tip.

Pereopod-3 (**Figure 13A**) basis broken; ischium with ventrodistal seta; merus 1.8 L:W, 0.7× carpus, with ventrodistal seta; carpus 2.7 L:W, 0.8× propodus, with two ventrodistal, short middistal, and long (0.8× propodus) dorsodistal setae; propodus 4.5 L:W, 1.0× dactylus and unguis combined, with spinules near dactylus insertion and ventrosubdistal seta; dactylus 0.8× unguis, unarmed; unguis unarmed, with rounded tip.

Pereopod-4 (**Figure 13B**) coxa with seta; basis 5.3 L:W, 3.6× merus, with two penicillate ventral setae; ischium with two ventrodistal setae; merus 2.0 L:W, 0.8× carpus, with two ventrodistal setae; carpus 2.4 L:W, 1.0× propodus, with one short dorsodistal and two long ventrodistal setae; propodus 3.4 L:W, 0.6× dactylus and unguis combined, with two ventrodistal, one dorsodistal setae; dactylus 0.4× unguis, unarmed; unguis unarmed, with rounded tip.

Pereopod-5 (**Figure 13C**) similar to pereopod-4.

Pereopod-6 (**Figure 13D**) similar to pereopod-4, but basis with one midventral and one middorsal penicillate setae, and ischium with ventrodistal seta.

Pleopods absent

Uropod (**Figure 13E**) exopod reduced and fused with the basal article, endopod one-articled, 1.2 L:W, with two subdistal and four distal setae.

Description of juvenile male: Body and appendages from paratype (NMV J 74725). BL = 2.5 mm. Body (**Figures 11C,D**) 7.5 L:W. Carapace 1.2 L:W, 0.2× BL. Pereonites 0.6× BL, pereonites 1-6: 0.6, 1.0, 1.3, 1.8, 1.5, and 0.8 L:W, respectively. Pleon combined with pleotelson 0.2× BL. Pleonites 0.2 L:W each. Pleotelson 1.4× pleonites 5–6.

Labium (**Figure 13F**) with the spiniform distal process (broken, not figured) and lateral process, covered by numerous setae.

Maxilliped (**Figure 13G**) palp article-1 rectangular, with proximal seta; article-2 1.8 L:W, with three inner plumose setae; article-3 2.2 L:W, with three inner plumose setae; article-4 left palp 1.3 L:W, with five inner plumose distal setae; article-4 right palp 1.4 L:W, with four inner plumose setae distally. Basis covered with numerous setae of different lengths, with rounded distal projection, minute seta near palp insertion.

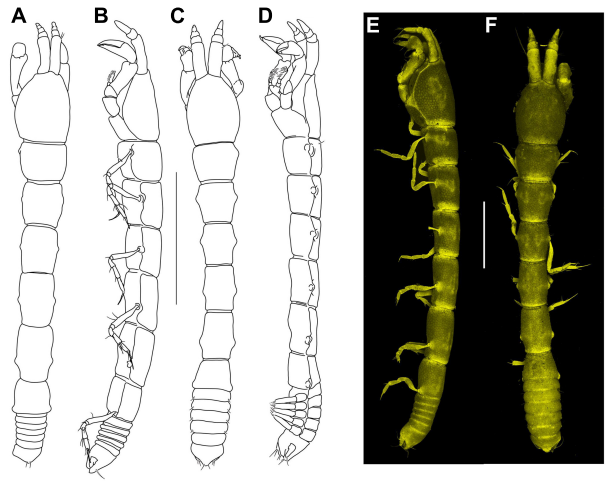

FIGURE 14 | *Agathotanais paleroi* n. sp., neuter, holotype (**A,B**: ZMH K-61175), juvenile male, paratype (**C,D**: NHM 58023), neuter, paratype (**E,F**: ZMH K-61178). **(A)** Dorsal view; **(B)** lateral view; **(C)** dorsal view; **(D)** lateral view; **(E)** lateral view (confocal picture); **(F)** dorsal view (confocal picture). Scale bars: **(A–D)** = 1 mm, **(E,F)** = 500 μm.

Epignath (**Figure 13H**) narrow, curved, with terminal robust plumose seta.

Cheliped (**Figure 13I**) basis 1.2 L:W, naked; merus with midventral seta; carpus 2.8 L:W, marginally shorter than propodus and fixed finger combined, with two midventral setae; palm 1.2 L:W, with seta near dactylus insertion and a row of ventral setae; fixed finger as long as palm, with one ventral seta, cutting edge with two tubercles and three setae; dactylus as long as a fixed finger, curved, naked; unguis moderate size.

Intraspecific variation: Juvenile male: maxilliped palp article-4 with four-five distal setae on the left and right palp, respectively.

Distribution: SE Australian coast, off Bermagui, East Gippsland (**Figure 2**); depth range: 4064–4744 m.

Remarks. *Agathotanais oharai* belongs to the group of *Agathotanais* with a short cheliped palm (L:W 1.0–1.2), together with *A. ghilarovi*, *A. splendidus*, and *A. paleroi* (**Table 1**). It differs from *A. paleroi* in the unguis of pereopod-6, which is unarmed in *A. oharai* and serrated in *A. paleroi*. Additionally *A. oharai* has a pleon narrower than pereonite-6, what distinguishes it from *A. splendidus* and *A. ghilarhovi*, which have the pleon as wide as peronite-6 (**Table 1**).

***Agathotanais paleroi* n. sp. Stępień, Jakiel and Błażewicz.**

This species is register under the zoobank number:
LSIDurn:lsid:zoobank.org:act:05C2DC1B-33B8-492F-B319-FA70B2FE0C22

(**Figures 14–16**)

Material examined: Holotype: neuter, 3.0 mm, KuramBio st. 2-9, (ZMH K-61175).

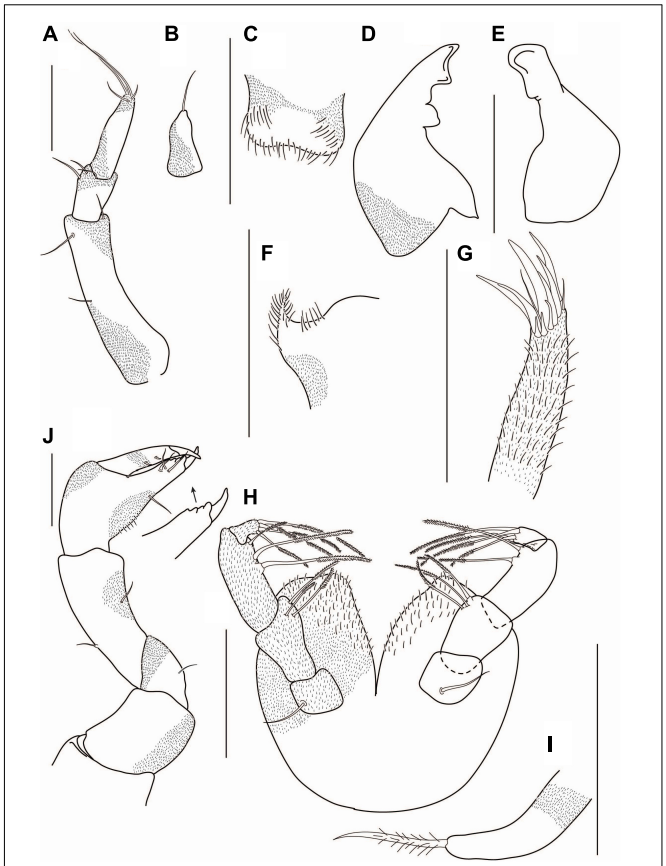

FIGURE 15 | *Agathotanais paleroi* n. sp., neuter, paratype (**A,C,F,J**: NHM 58022; **B,D,E,G–I**: ZMH K-61177). **(A)** antennule; **(B)** antenna; **(C)** labrum; **(D)** left mandible; **(E)** right mandible; **(F)** labium; **(G)** maxillule; **(H)** maxilliped; **(I)** epignath; **(J)** cheliped. Scale bars: **(A–I)** = 10 μm, **(J)** = 100 μm.

Paratypes: juvenile male, 3.5 mm, KuramBio st. 2-10, (NHM 58023); neuter, dissected on slides, 3.0 mm, KuramBio st. 5-10, (NHM 58022); juvenile male dissected on slides, 2.9 mm, KuramBio st. 2-9, (ZMH K-61176); juvenile male, 2.4 mm, KuramBio st. 2-10, (NHM 58024); neuter, 3.1 mm, KuramBio st. 2-9, (NHM 58025); neuter, 2.6 mm, KuramBio st. 5-9, (NHM 58026); neuter, 2.9 mm, KuramBio st. 6-11, (ZMH K-61178); manca II, 1.4 mm, KuramBio st. 8-12, (ZMH K-61179); manca III, 1.8 mm, KuramBio st. 8-12, (ZMH K-61179); neuter, 2.8 mm, KuramBio st. 8-12, (ZMH K-61179); neuter, 2.8 mm, KuramBio st. 8-9, (NHM 58027); neuter, 3.1 mm, partly dissected on slide, KuramBio st. 1-11, (ZMH K-61177); neuter, 2.3 mm, KuramBio st. 8-1, (NHM 58028); manca III, 1.9 mm, KuramBio st. 8-1, (NHM 58029); neuter, 3.2 mm, KuramBio st. 6-12, (NHM 58030); neuter, broken, KuramBio st. 5-9, (NHM 58031); neuter, 3.2 mm, KuramBio st. 3-9, (NHM 58032); two neuters, broken, KuramBio st. 2-9, (ZMH K-61180); manca, broken, KuramBio st. 5-10, (ZMH K-61181); neuter, broken, KuramBio st. 5-9, (ZMH K-61182).

Diagnosis of neuter: Body narrow (7.0 L:W). Carapace without pair of lateral setae in posterior margin. Pereonite-1 without pair of dorsal setae. Pereonites 4–6 longer than

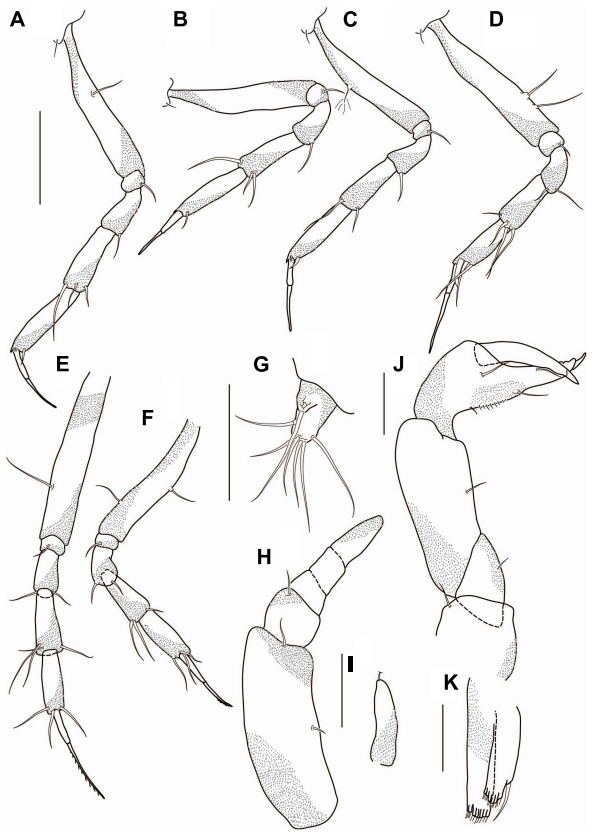

FIGURE 16 | *Agathotanais paleroi* n. sp., neuter, paratype (**A–G**: NHM 58022), juvenile male, paratype (**H–K**: ZMH K-61176). **(A)** Pereopod-1; **(B)** pereopod-2; **(C)** pereopod-3; **(D)** pereopod-4; **(E)** pereopod-5; **(F)** pereopod-6; **(G)** uropod; **(H)** antennule; **(I)** antenna; **(J)** cheliped; **(K)** pleopod. Scale bar: **(A–G)** = 100 μm.

wide. Pereonite-6 similar in length to pleonites 1–5 combined. Pleonites 1–5 narrower than pereonite-6. Antennule article-1 longer than the remaining articles combined, about 2.0× article-3. Antenna one-articled. Cheliped palm as long as wide. Pereopods 2–3 carpus with dorsodistal seta 0.7× propodus. Pereopod 4 unguis unarmed, pereopods 5–6 unguis with serration. Uropod endopod one-articled.

Etymology: Species is dedicated to Dr. Ferran Palero (University of Valencia), a great colleague, fellow, and peracarid specialist.

Description of neuter: Body from the holotype (ZMH K-61175), appendages from paratypes (NHM 58022 and ZMH K-61177). BL = 3 mm. Body (**Figures 14 A,B,E,F**) 7.0 L:W, elongated. Carapace 1.2 L:W, 0.1× BL, with rounded lateral margins. Pereon 0.7× BL, pereonites 1–6: 0.7, 1.0, 1.2, 1.5, 1.6, and 0.9 L:W, respectively, all pereonites rectangular. Pleon with pleotelson 0.1× BL. Pleonites 1–5 0.1 L:W each.

Antennule (**Figure 15A**) article-1 4.5 L:W, 3.0× article-2, with one midlength, one subdistal and one distal seta; article-2 1.5 L:W, 0.6× article-3, with three outer subdistal setae; article-3 3.5 L:W, with two short subdistal and two long distal setae.

Antenna (**Figure 15B**) one-articled, 2.0 L:W, subtriangular, tipped with seta.

Mouthparts: Labrum (**Figure 15C**) hood-shaped, covered with numerous setae of different lengths.

Left mandible (**Figure 15D**) incisor with two blunt teeth, *lacinia mobilis* rounded and short-fused with incisor.

Right mandible (**Figure 15E**) incisor with blunt tooth distally.

Labium (**Figure 15F**) with a spiniform distal process (broken, not pictured) and lateral process, covered by numerous setae.

Maxillule endite (**Figure 15G**) with ten distal spines and distal fine setae of different lengths.

Maxilliped (**Figure 15H**) palp article-1 rectangular, with proximal seta; article-2 1.8 L:W, with three inner plumose setae; article-3 2.3 L:W, with three inner plumose setae (one hidden under the article-4); article-4 1.8 L:W, with four distal plumose setae. Basis rounded, covered by numerous setae of different lengths.

Epignath (**Figure 15I**) elongated, tipped with plumose setae.

Cheliped (**Figure 15J**) basis 1.0 L:W, naked; merus with midventral seta; carpus 2.6 L:W, marginally shorter than propodus and fixed finger combined, with one middorsal and one midventral setae; palm 1.0 L:W, with seta near dactylus insertion and with a row of setae ventrally; fixed finger similar in length to palm, with midventral seta, cutting edge with tubercles and three setae, terminal spine sharp; dactylus as long as a fixed finger, cutting edge with two spines; unguis slender.

Pereopod-1 (**Figure 16A**) coxa with seta, basis 5.5 L:W, 4.5× merus, with midventral seta; ischium with ventrodistal seta; merus 1.3 L:W and 0.4× carpus, with ventrodistal seta; carpus 2.7 L:W, 0.8× propodus, with two short ventrodistal and long (0.7× propodus) dorsodistal setae; propodus 1.7 L:W, 1.0× dactylus and unguis combined, with spinules near dactylus insertion and ventrodistal seta; dactylus 0.7× unguis, unarmed; unguis unarmed, with rounded tip.

Pereopod-2 (**Figure 16B**) coxa with seta; basis 5.0 L:W, 3× merus, naked; ischium with ventrodistal seta; merus 2.0 L:W, 0.5× carpus, with ventrodistal seta; carpus 2.8 L:W, 0.8× propodus, with two ventrodistal and long (0.7× propodus) dorsodistal setae; propodus 3.8 L:W, 1.2× dactylus and unguis combined, with spinules near dactylus insertion and ventrodistal seta; dactylus 0.8× unguis, unarmed; unguis unarmed, with rounded tip.

Pereopod-3 (**Figure 16C**) coxa with seta; basis 5.8 L:W, 3.3× merus, with penicillate middorsal seta; ischium with ventrodistal seta; merus 2.0 L:W, 0.5× carpus, with ventrodistal seta; carpus 2.8 L:W, 0.8× propodus, with ventrodistal seta and long (0.7× propodus) dorsodistal seta; propodus 5.0 L:W, 1.0× dactylus and unguis combined, with spinules near dactylus insertion and ventrodistal seta; dactylus 0.5× unguis, unarmed; unguis unarmed, with rounded tip.

Pereopod-4 (**Figure 16D**) coxa with seta; basis 5.0 L:W, 3.8× merus, with two midventral seta; ischium with ventrodistal seta; merus 1.6 L:W, 0.7× carpus, with two ventrodistal setae; carpus 2.3 L:W, 1.0× propodus, with three long dorsodistal and one short ventrodistal setae; propodus 2.7 L:W, 0.6×

dactylus and unguis combined, with two simple and one robust dorsodistal setae; dactylus 0.4× unguis, unarmed; unguis unarmed, with rounded tip.

Pereopod-5 (**Figure 16E**) basis 5.1 L:W, 3.4× merus, with midventral seta; ischium with middistal seta; merus 2.2 L:W, 0.7× carpus, with two distal setae; carpus 2.6 L:W, 1.0× propodus, with four distal setae; propodus 3.2 L:W, 0.6× dactylus and unguis combined, with two ventrodistal, one dorsodistal setae; dactylus 0.5× unguis, unarmed; unguis serrated ventrally.

Pereopod-6 (**Figure 16F**) basis 5.2 L:W, 3.4× merus, with one ventral and one dorsal setae; ischium with middistal seta; merus 1.6 L:W, 0.6× carpus, with two ventrodistal setae; carpus 2.2 L:W, 1.0× propodus, with two ventrodistal and one dorsodistal setae; propodus 2.4 L:W, 0.7× dactylus and unguis combined length, with two ventrodistal one dorsodistal setae; dactylus 0.8× unguis, dactylus unarmed; unguis serrated ventrally.

Pleopods absent.

Uropod (**Figure 16G**) exopod reduced and fused with the basal article, tipped with two setae (one broken); endopod one-articled, with four distal and two subdistal setae.

Description of the juvenile male: Body from paratype (NHM 58023), appendages from paratype (ZMH K-61176). BL = 3.5 mm. Body elongated (**Figures 15 C,D**) 7.4 L:W. Carapace 1.3 L:W, 0.9× pereonites 1–2, 0.1× BL. Pereonites 0.7× BL, pereonites 1–6: 0.7, 1, 1.1, 1.4, 1.3, and 0.7 L:W, respectively, last pereonite trapezoidal in dorsal view. Pleon combined with pleotelson 0.1× BL. Pleonites 0.2 L:W. Pleotelson 0.7× pleonites 4–5.

Antennule (**Figure 16H**) with five articles; article-1 2.7 L:W, 1.6× article-2, with one midlength and one distal seta; article-2 0.8 L:W, 0.3× article-3, with distal seta; article-3 0.5 L:W, naked, article-4 0.7 L:W, naked, article-5 2.3 L:W, naked.

Antenna (**Figure 16I**) one-articled, 3.4 L:W, tipped with a seta.

Cheliped (**Figure 16J**) basis 1.0 L:W, with the dorsodistal seta; merus with midventral seta; carpus 2.5 L:W, 1.6× palm, with midventral seta; chela palm 1.5 L:W, with seta near dactylus insertion and with row of ventral setae; fixed finger with ventral seta, cutting edge with two inner setae, and with three tubercles distally, distal spine sharp; dactylus as long as a fixed finger; unguis slender.

Pleopod (**Figure 16K**) exopod with six distal and one subdistal setae; endopod with eight setae.

Intraspecific variation: Manca III: length 1.8–1.9 mm.

Neuter: length 2.3–3.2 mm; antenna article-1 with zero/one midlength seta; cheliped carpus with one/two midventral setae.

Juvenile male: length 2.4–2.9 mm; cheliped fixed finger cutting edge with one/three inner setae.

Distribution: NW Pacific, Kuril-Kamchatka Trench (**Figure 2**); depth range: 4976–5388 m.

Remarks. *Agathotanais paleroi* n. sp., collected from the KKT, belongs to the species of *Agathotanais* with a short cheliped palm (L:W 1.0–1.2). It differs from other short-palm species by the appearance of the unguis of pereopod-6: serrated in *A. paleroi* but unarmed in *A. ghilarovi*, *A. splendidus*, and *A. oharai*. Furthermore, *A. paleroi* has a pleon narrower than pereonite-6, distinguishing it from *A. splendidus* and *A. ghilarhovi* with a pereonite-6 that is as wide as pleon (**Table 1**).

***Agathotanais* sp. abyss-1**.

(**Supplementary Figures 1, 2**)

Material examined: Neuter, 3.3 mm, dissected on the slides, ABYSS st. 9, (NMV J 74664).

Description of neuter: BL = 3.3 mm. Body (**Supplementary Figures 1A,B**) 7.7 L:W. Carapace 1.2 L:W, 0.1× BL, with pair of lateral posterior setae. Pereon 0.7× BL, pereonites 1–6: 0.8, 1.0, 1.3, 1.6, 2.0, and 1.4 L:W, respectively, all pereonites rectangular in dorsal view. Pleon with pleotelson 0.1× BL. Pleonites 1–5 0.3 L:W each. Pleotelson in dorsal view 0.8× pleonites 1–5.

Antennule (**Supplementary Figure 1C**) article-1 3.8 L:W, 4.7× article-2, with three inner setae: one midlength and three subdistal setae; article-2 1.2 L:W, 0.5× article-3, with two subdistal setae; article-3 3.3 L:W, with three long and one short distal setae.

Antenna (**Supplementary Figure 1D**) one-articled, 2.0 L:W, tipped with a seta.

Mouthparts: Labrum (**Supplementary Figure 1E**) rounded, with numerous setae of different lengths.

Left mandible (**Supplementary Figure 1F**) incisor with two blunt teeth, *lacinia mobilis* small and fused with incisor.

Right mandible (**Supplementary Figure 1G**) incisor with a blunt tooth.

Labium (**Supplementary Figure 1H**) with a spiniform distal process (broken, not pictured) and lateral process, covered by numerous setae.

Maxillule endite (**Supplementary Figure 1I**) with eleven distal spines of different lengths.

Maxilliped (**Supplementary Figure 1J**) palp article-1 broken; article-2 2.2 L:W, with three inner plumose setae, article-3 2.6 L:W, with three inner plumose setae, article-4 1.6 L:W, with five subdistal and distal setae, and one short outer seta.

Epignath (**Supplementary Figure 1K**) elongated, tipped with a plumose seta.

Cheliped (**Supplementary Figure 2A**) basis 1.0 L:W, naked, rectangular; merus with midventral seta; carpus 2.2 L:W, marginally shorter than propodus and fixed finger combined, with two midventral, one dorsoproximal, and one dorsosubdistal setae; chela palm 1.4 L:W, with seta near dactylus insertion and with row of ventral setae; fixed finger 0.8× palm, cutting edge with three setae; dactylus as long as a fixed finger, cutting edge with short proximal seta.

Pereopod-1 (**Supplementary Figure 2B**) coxa with seta; basis 6.0 L:W, 3.7× merus, naked; ischium with ventrodistal seta; merus 1.6 L:W and 0.5× carpus, with two ventrodistal seate; carpus 3.3 L:W, 0.7× propodus, with two ventrodistal and long (0.5× propodus) dorsodistal setae; propodus 6.6 L:W, with projection near dactylus insertion, and with ventrodistal seta; dactylus unarmed; unguis is broken.

Pereopod-2 (**Supplementary Figure 2C**) coxa with seta; basis 7.5 L:W, 4.0× merus, with penicillate middorsal seta; ischium with ventrodistal seta; merus 1.7 L:W, 0.8× carpus, with ventrodistal seta; carpus 2.2 L:W, 0.6× propodus, with

two ventrodistal and long (0.7× propodus) dorsodistal setae; propodus 4.8 L:W, 1.0× dactylus and unguis combined, with projection near dactylus insertion, and with ventrodistal seta; dactylus 0.7× unguis, unarmed; unguis unarmed, with rounded tip.

Pereopod-3 (**Supplementary Figure 2D**) coxa with seta; basis 6.0 L:W, 3.4× merus, naked; ischium naked; merus 1.7 L:W, 0.6× carpus, with ventrodistal seta; carpus 3.3 L:W, 0.8× propodus, with ventrodistal and dorsodistal setae; propodus 4.8 L:W, 1.0× dactylus and unguis combined length, with subdistal seta; dactylus 0.6× unguis, unarmed; unguis unarmed, with rounded tip.

Pereopod-4 missing.

Pereopod-5 (**Supplementary Figure 2E**) coxa with seta; basis 5.6 L:W, 5.0× merus, with penicillate middorsal seta; ischium with two ventrodistal setae; merus 1.3 L:W, 1.0× carpus, with ventrodistal seta; carpus 2.6 L:W, 1.0× propodus, with two ventrodistal and one dorsodistal setae; propodus 3.5 L:W, 0.7× dactylus and unguis combined, with two ventrodistal and one dorsodistal setae; dactylus 0.4× unguis, unarmed; unguis unarmed, with rounded tip.

Pereopod-6 (**Supplementary Figure 2F**) coxa with seta; basis 6.0 L:W, 4.8× merus, with penicillate midventral seta; ischium with ventrodistal seta; merus 1.6 L:W, 0.7× carpus, with ventrodistal seta, dorsodistal seta not seen; carpus 2.3 L:W, 1.0× propodus, with two ventrodistal setae; propodus 3.0 L:W, 0.7× dactylus and unguis combined, with two ventrodistal and one dorsodistal setae; dactylus 0.4× unguis, unarmed; unguis unarmed, with rounded tip.

Pleopods absent.

Uropod (**Supplementary Figure 2G**) exopod reduced and fused with basal article, tipped with seta; endopod one-articled, 2.2 L:W, with two distal setae.

Distribution: SE Australia, off the Tasmanian coast, Freycinet Marine Park (**Figure 2**); depth range: 4021–4035 m.

Remarks: *Agathotanais* sp. abbys-1 belongs to the species of *Agathotanais* with a moderate elongated cheliped palm (L:W 1.3–1.4) (**Table 1**). It differs from *A. beatae* by an unarmed pereopod-4 unguis (serrated in *A. beatae*). Moreover, in *Agathotanais* sp. abbys-1 the pleonites are narrower than pereonite-6, whereas in *A. beatae* they are similar in width. On the other hand, it can be distinguished from *A. manganicus* by a one-articled antenna (two-articled in *A. manganicus*). Finally, *Agathotanais* sp. abbys-1 differs from *A. spinipoda* by the propodus of pereopod-6. It is smooth in *Agathotanais* sp. abyss-1 but has a row of spines in *A. spinipoda* (**Table 1**).

Agathotanais indet.

Additional material: *Agathotanais* indet: poor condition, st. 9, NMV74664. SE Pacific, Tasmania coast, Freycinet Marine Park; depth range: 4021–4035 m.

DISCUSSION

The Pacific is a vast ocean with a high variety of benthic environments and ecosystems (Gage and Tyler, 1991). Many of its regions have never been explored, and its fauna and diversity remain simply unknown. This deficient biological recognition is particularly evident when it comes to the identification of a group of organisms that is particularly poorly understood (Błażewicz-Paszkowycz and Bamber, 2012) and it is seen in the proportion of the new taxa discovered (e.g., Larsen and Shimomura, 2007; Błażewicz-Paszkowycz et al., 2013; Bird, 2015; Jakiel et al., 2019, 2020). This work presented findings on just one genus of small macrobenthic peracarids, which was collected from several locations of the North Pacific. Only two of eight identified species were previously described, regardless of the fact that some areas had been previously investigated, e.g., the KKT (Larsen, 2007; Larsen and Shimomura, 2007) or the Clarion Clipperton Fracture Zone (Larsen, 1999). As a result of our study, the number of species known from the Pacific has raised from five to ten, and the total number of species classified into this genus increases from 12 to 17.

Phylogenetic and Genetic Analyses

The current research presents the first results from studies on the extensive collections of *Agathotanais* performed in the frame of an integrative taxonomy approach, combining molecular and morphological techniques. So far, only five agathotanaid sequences were deposited at GenBank and only two of them were identified down to species level — *A. ingolfi* (Błażewicz-Paszkowycz et al., 2014). In the present study, we upgrade the number of sequences to 12, adding three fragments of 18S from species: *A. frutosae*, *A. jani,* and *A. paleroi*, and four H3 sequences from *A. frutosae*, *A. oharai, A. paleroi,* and *Agathotanais* sp. abyss-1. These results, based on two markers, should be considered merely as the first step into more complex phylogenetic studies in the future. Nevertheless, the results allow us to confirm the monophyletic character of *Agathotanais*, as well as of another agathotanaid genus — *Paragathotanais.* Moreover, both genera grouped within the same clade in both obtained phylogenetic trees, confirming their close relationship, although for full phylogenetic resolution and testing of the monophyletic character of Agathotanaidae more genetic data including also other genera are needed.

Within the *Agathotanais*, *A. oharai* from the Australian slope and *Agathotanais* sp. abbys-1 from the Tasmanian slope showed a close relationship (**Figure 1**). Both species present similar body appearance, with similar sizes, a gently rounded lateral margin of the carapace, pereonites rectangular in dorsal view. They both reveal similar proportions of the antennule articles and ratios of length to width in antenna and uropod. The next similarities are the appearance of the pereopods, with elongated carpus and propodus in pereopods 1–3 and unarmed unguis in pereopods 4–6. The molecular and morphological similarities of both species are

supported by a relatively small geographic distance between their known distributions.

Agathotanais oharai and *Agathotanais* sp. abbys-1 were located on the tree close to *A. paleroi*. *Agathotanais paleroi* is separated by several thousands of kilometers from the two species *A. oharai* and *Agathotanais* sp. abbys-1. The taxonomical characters that support genetic similarities are the appearance of the cheliped and the length of the distroventral setae on pereopods 2–3. All three species are characterized by a short or moderately short cheliped palm (L:W less than 1.4) and long dorsodistal setae on the carpus of pereopods 2 and 3 (0.7–0.8× propodus). These features distinguish these species from *A. frutosae*, with a long cheliped palm (1.6 L:W) and short setae on the carpus (0.4–0.6× propodus). Moreover, *A. frutosae* bears a pair of setae on the dorsal surface of the first pereonite, a character that is unique among *Agathotanais* species. The pereopods of *A. frutosae* are thicker and armed with strong setae (e.g., carpus and propodus of pereopods 1–3). The place of occurrence of *A. frutosae* – a semi-enclosed sea – may influence the isolation of the species and the evolution of characters different from other *Agathotanais* species.

Distribution

The genus *Agathotanais* is a cosmopolitan taxon. It was recorded in temperate and tropical zones of the Atlantic, Indian, and Pacific Oceans (Kakui and Kohtsuka, 2015; Chim and Tong, 2021). So far, the genus is absent only from the south of the Antarctic Polar Front (Błażewicz-Paszkowycz and Siciński, 2014; Pabis et al., 2014), although one undescribed species of *Agathotanais* was registered for the slope of the Scotia Sea (Pabis et al., 2015). Since the slope and the abyssal zone of the Southern Ocean are vast and still unexplored areas (Brandt et al., 2007) it can be assumed that the distribution of *Agathotanais* in the Antarctic may be wider, although yet to be discovered.

Regardless of the wide zoogeographical distribution of the genus, each species of *Agathotanais* usually has a narrow zoogeographical range (with the exception of *A. hanseni* and *A. ingolfi*; see Kakui and Kohtsuka, 2015; Chim and Tong, 2021). They are often limited to a defined basin (e.g., sea or trench), although in the case of *A. jani* the boundary is not physically obvious. That species was, however, present only at the closest stations of the Central Pacific (CCZ), separated by a maximal distance of less than 1,000 km (**Figure 2**). The mechanisms which support the connectivity in deep-sea populations are not fully understood yet. The data on population genetics combined with biophysical transport models and trace-element signatures that scrutinized the dispersal potential of deep-sea fauna is just one order of magnitude larger than for shallow water fauna (Baco et al., 2016). Those findings question the paradigm of unlimited distribution of deep-sea species. It is not clear how tube-building small tanaids can sustain genetic connectivity for their low numbers and sparsely distributed populations. The presence in the deep-sea population of mobile males "swimming" (Błażewicz-Paszkowycz et al., 2014) along with favorable hydrological regimes and near-bottom currents adds to the rationale of this phenomenon, although it does not explore the problem. Moreover, neither physical nor hydrological connections warrant an unlimited distribution. *A. frutosae* is known from the Sea of Okhotsk, isolated from the open Pacific by the Kuril Islands. Although hydrological contact between the sea and the Pacific is sustained by numerous straits (Bussol Strait is 2,300 m deep), they do not perform as a zoogeographical passage that would allow the species to disperse.

Depth Ranges

Agathotanais is considered a deep-water genus (Kudinova-Pasternak, 1970, 1989, 1990; Larsen, 2007), which mainly occurs below continental shelf depths; hence their lack of eyes supports a deep-sea origin. In the North West and Central Pacific, they occur between 3,400 and 5,500 m (e.g., Larsen, 1999; Kakui and Kohtsuka, 2015; Chim and Tong, 2021), but three species, two off Japan (*A. toyoshioae*; *A. misakiensis*) and one-off SE Australia (*A. spinipoda* Larsen, 1999), were found on the shelf (95 m; 200–493 m) and the slope 400–1,840 m, respectively (Larsen, 1999; Kakui and Kohtsuka, 2015).

Abundances

Food availability is an essential factor that shapes the diversity in the oceans. The heterotrophic deep-sea fully depends on the external source of the energy that is produced on land or in the photic zone of the ocean. The flux of particulate organic matter (POM) to the seafloor declines in the bathyal and abyssal zones; hence, the coastal oceanic regions are more productive and sustain higher diversity than the open ocean (Woolley et al., 2016; Sweetman et al., 2017). A high primary productivity driven by complex hydrological conditions (Nürnberg and Tiedemann, 2004) justifies the high abundances of *A. frutosae* in the western and deeper part of the Sea of Okhotsk (22% of all collected tanaids; Stępień et al., 2019), observed also for other groups of the benthos, e.g., polychaetes, isopods, amphipods, diatoms (Artemova et al., 2018; Brandt et al., 2018a,b; Frutos and Jażdżewska, 2019). Despite *A. frutosae* being recorded on both sides of Kuril Island, its distribution range was limited to stations of similar depth (about 3000 m), physical parameters (salinity, temperature), and relatively high amounts of carbon in the sediment (Stępień et al., 2019).

Agathotanais frutosae has been collected only inside the Sea of Okhotsk, although the hydrological connectivity between the sea and adjacent basins is sustained. It absent from the neighboring Sea of Japan (Błażewicz-Paszkowycz et al., 2013) as well as from deeper (4,000–5,000 m) abyssal zones surrounding the Kuril-Kamchatka Trench (Kudinova-Pasternak, 1970; Larsen, 2007; Błażewicz et al., 2019). In the open oceanic waters of the North West Pacific, *Agathotanais* was represented by *A. paleroi* and *A. hadalis*. *Agathotanais paleroi* was identified in our studies through integrative methods. It was located on both sides of the

trench, similar to other tanaids and isopods (Lörz et al., 2018; Bober et al., 2019; Jakiel et al., 2019).

DATA AVAILABILITY STATEMENT

This article is registered in ZooBank number: urn:lsid:zoobank.org :pub:F17F01E3-5FF7-41A6-A7A7-6DA8277AA417.

AUTHOR CONTRIBUTIONS

AS: general concept, identification of the material (SokhoBio, KuramBio, ABYSS collection), description and figures of new species, and writing the manuscript. PJ: identification of the material (SO-239 collection), description and figures of new species, SEM images, and editing the manuscript. AJ: DNA and lab work, analysis of the molecular data, light microscope images, editing the figures, and editing the manuscript. AP: description and figures of new species. MB: general concept, identification of the material (SO-239, ABYSS collection), and editing the manuscript. All authors contributed to the article and approved the submitted version.

FUNDING

The material was collected and sorted within the framework of several large international projects. The KuramBio I and II projects and the SokhoBio project were financially supported by the German Ministry for Science and Education, grant 03G0857A, KuramBio I BMBF grant 03G0223A, as well as KuramBio II BMBF grant 03G0250A thanks to Angelika Brandt, Senckenberg Museum, Frankfurt, Germany. The projects were supported by the Russian Foundation of Basis Research (projects 13-04-02144, 16-04-01431), the Council of the President of the Russian Federation (project МК-2599.2013.4), Russian Federation Government Grant No. 11.G34.31.0010, grant of Presidium of the Far East Branch of RAS (12–I–P30–07), and Otto Schmidt Laboratory grant (OSL-14-15). Project ABYSS funding was provided by the Marine Biodiversity Hub, supported through the Australian Government's National Environmental Science Program (NESP). This work was also supported by NCN OPUS 2018/31/B/NZ8/03198.

ACKNOWLEDGMENTS

The materials from Central Pacific was collected in the framework of the Joint Programming Initiative Healthy and Productive Seas and Oceans (JPIOceans) project "Ecological Aspects of Deep-sea Mining" (project EcoResponse Assessing the Ecology, Connectivity, and Resilience of Polymetallic Nodule Field Systems–Chief scientist: Pedro Martínez Arbizu). The authors thank the crews of the RV *Sonne* and *Akademik M.A. Lavrentyev* for their help onboard and all student helpers and technicians for support and help with sorting of the extensive expedition material. The authors wish to thank the CSIRO Marine National Facility (MNF) for its support in the form of sea time on RV *Investigator,* including personnel, scientific equipment, and data management. The authors also thank all the scientific staff and crew who participated in voyage IN2017_V03. All data and samples acquired on the voyage are made publicly available in accordance with the MNF Policy. Special thanks to Emma Palacios Theil for linguistic corrections and Maciej Studzian for confocal images.

SUPPLEMENTARY MATERIAL

The Supplementary Material for this article can be found online at: https://www.frontiersin.org/articles/10.3389/fmars.2021.741536/full#supplementary-material

Supplementary Figure 1 | *Agathotanais* sp. abyss-1, neuter, (NMV J 74664). **(A)** Dorsal view; **(B)** lateral view; **(C)** antennule; **(D)** antenna; **(E)** labrum; **(F)** right mandible; **(G)** left mandible; **(H)** labium; **(I)** maxillule; **(J)** maxilliped; **(K)** epignath. Scale bar: **(A,B)** = 1 mm, **(C–K)** = 10 μm.

Supplementary Figure 2 | *Agathotanais* sp. abyss-1, neuter, (NMV J 74664). **(A)** cheliped; **(B)** pereopod-1; **(C)** pereopod-2; **(D)** pereopod-3; **(E)** pereopod-5; **(F)** pereopod-6; **(G)** uropod. Scale bar: **(A–G)** = 100 μm.

Supplementary Table 1 | Detailed information about deep-sea expeditions during which *Agathotanais* specimens were collected; Expeditions: SokhoBio, Sea of Okhotsk Biodiversity Studies; KuramBio, Kuril-Kamchatka Biodiversity Study; JPIO, European Joint Project Initiative Oceans; ABYSS, Sampling the abyss; SLOPE, campaign to continental slope of Bass Strait; MANGAN, expedition to CCZ under the framework of Ecological Aspects of Deep Sea Mining; License Areas: BGR, Bundesanstalt fur Geowissenschaften und Rofstoffe, Germany; IOM, Interoceanometal Joint Organisation; GSR, Global Sea Mineral Resources NV, Belgium; APEI3, Areas of Particular Environmental Interest 3; Gear: EBS, epibenthic sledge; S, supranet; E, epinet; BC, box corer.

Supplementary Table 2 | Pairwise genetic distances between agathotanaids species for H3 and 18S sequences.

Supplementary Material | Key for *Agathotanais* species.

REFERENCES

Altschul, S. F., Gish, W., Miller, W., Myers, E. W., and Lipman, D. J. (1990). Basic local alignment search tool. *J. Mol. Biol.* 215, 403–410. doi: 10.1016/S0022-2836(05)80360-2

Artemova, A. V., Sattarova, V. V., and Vasilenko, Y. P. (2018). Distribution of diatoms and geochemical features of holocene sediments from the Kuril Basin (Sea of Okhotsk). *Deep Sea Res. Part II Top. Stud. Oceanogr.* 154, 10–23.

Baco, A. R., Etter, R. J., Ribeiro, P. A., der Heyden, S., Beerli, P., and Kinlan, B. P. (2016). A synthesis of genetic connectivity in deep-sea fauna and implications for marine reserve design. *Mol. Ecol.* 25, 3276–3298. doi: 10.1111/mec.13689

Bird, G. J. (2015). Tanaidacea (Crustacea) of the kermadec discovery expedition 2011, with a new sub-family of paratanaidae: metatanainae. *Bull. Auckland Mus.* 20, 369–404.

Bird, G. J., and Holdich, D. M. (1988). Deep-sea Tanaidacea (Crustacea) of the North-East Atlantic: the tribe Agathotanaini. *J. Nat. Hist.* 22, 1591–1621. doi: 10.1080/00222938800771001

Blaxter, M. L., De Ley, P., Garey, J. R., Llu, L. X., Scheldeman, P., Vierstraete, A., et al. (1998). A molecular evolutionary framework

for the phylum Nematoda. *Nature* 392, 71–75. doi: 10.1038/32160

Błażewicz, M., Jakiel, A., Bamber, R. N., and Bird, G. J. (2021). Pseudotanaidae Sieg, 1976 (Crustacea: Peracarida) from the Southern Ocean: diversity and bathymetric pattern. *Eur. Zool. J.* 88, 1–76.

Błażewicz, M., Jóźwiak, P., Menot, L., and Pabis, K. (2019). High species richness and unique composition of the tanaidacean communities associated with five areas in the Pacific polymetallic nodule fields. *Prog. Oceanogr.* 176:102141. doi: 10.1016/j.pocean.2019.102141

Błażewicz-Paszkowycz, M., and Bamber, R. N. (2012). The shallow-water Tanaidacea (Arthropoda: Malacostraca: Peracarida) of the Bass Strait, Victoria, Australia (other than the Tanaidae). *Mem. Mus. Vic.* 69, 1–235. doi: 10.24199/j.mmv.2012.69.01

Błażewicz-Paszkowycz, M., Bamber, R. N., and Jóźwiak, P. (2013). Tanaidaceans (Crustacea: Peracarida) from the SoJaBio joint expedition in slope and deeper waters in the Sea of Japan. *Deep Sea Res. Part II Top. Stud. Oceanogr.* 8, 181–213. doi: 10.1016/j.dsr2.2012.08.006

Błażewicz-Paszkowycz, M., Jennings, R. M., Jeskulke, K., and Brix, S. (2014). Discovery of swimming males of Paratanaoidea (Tanaidacea). *Pol. Polar Res.* 35, 415–453. doi: 10.2478/popore-2014-0022

Błażewicz-Paszkowycz, M., and Siciński, J. (2014). Diversity and distribution of Tanaidacea (Crustacea) along the Victoria Land Transect (Ross Sea. Southern Ocean). *Pol. Biol.* 37, 519–529. doi: 10.1007/s00300-014-1452-7

Bober, J., Brandt, A., Frutos, I., and Schwentner, M. (2019). Diversity and distribution of Ischnomesidae (Crustacea: Isopoda: Asellota) along the Kuril-Kamchatka Trench – A genetic perspective. *Prog. Oceanog.* 178:102174. doi: 10.1016/j.pocean.2019.102174

Brandt, A., Alalykina, I., Fukumori, H., Golovan, O., Kniesz, K., Lavrenteva, A., et al. (2018a). First insights into macrofaunal composition from the SokhoBio expedition (Sea of Okhotsk, Bussol Strait and northern slope of the Kuril-Kamchatka Trench). *Deep Sea Res. Part II Top. Stud. Oceanogr.* 154, 106–120. doi: 10.1016/j.dsr2.2018.05.022

Brandt, A., and Barthel, D. (1995). An improved supra- and epibenthic sledge for catching Peracarida (Crustacea, Malacostraca). *Ophelia* 43, 15–23. doi: 10.1080/00785326.1995.10430574

Brandt, A., Frutos, I., Bober, S., Brix, S., Brenke, N., Guggolz, T., et al. (2018b). Composition of abyssal macrofauna along the Vema Fracture Zone and the hadal Puerto Rico Trench, northern tropical Atlantic. *Deep Sea Res. Part II Top. Stud. Oceanogr.* 148, 35–44. doi: 10.1016/j.dsr2.2017.07.014

Brandt, A., Gooday, A. J., Brandão, S. N., Brix, S., Brökeland, W., Cedhagen, T., et al. (2007). First insights into the biodiversity and biogeography of the Southern Ocean deep sea. *Nature* 447, 307–311. doi: 10.1038/nature05827

Chim, C. K., and Tong, S. J. W. (2021). Three new species of agathotanaids (Tanaidacea: Paratanaoidea: Tanaidomorpha) from the lower bathyal zone off southwestern Java, Indonesia, Indian Ocean with notes on the global distribution and diversity of Agathotanaidae. *Zootaxa* 5004, 067–106. doi: 10.11646/zootaxa.5004.1.3

Coleman, C. O. (2003). Digital inking: how to make perfect line drawings on computers. *Org. Divers. Evol.* 3, 303–304. doi: 10.1078/1439-6092-00081

Colgan, D., McLauchlan, A., Wilson, G. D., Livingston, S., Edgecombe, G., Macaranas, J., et al. (1998). Molecular phylogenetics of the Arthropoda: relationships based on histone H3 and U2 snRNA DNA sequences. *Aust. J. Zool.* 46, 419–437.

Dana, J. D. (1849). Conspectus crustaceorum. conspectus of the crustacea of the exploring expedition. *Am. J. Sci.* 8, 424–428.

Drummond, A. J., and Rambaut, A. (2007). BEAST: bayesian evolutionary analysis by sampling trees. *BMC Evol. Biol.* 7:214. doi: 10.1186/1471-2148-7-214

Drummond, A. J., Suchard, M. A., Xie, D., and Rambaut, A. (2012). Bayesian phylogenetics with BEAUti and the BEAST 1.7. *Mol. Biol. Evol.* 29, 1969–1973. doi: 10.1093/molbev/mss075

Frutos, I., Brandt, A., and Sorbe, J. C. (2016). "Deep-sea suprabenthic communities: the forgotten biodiversity," in *Marine Animal Forests*, eds S. Rossi, L. Bramanti, A. Gori, and C. Orejas Saco del Valle (Cham: Springer International Publishing), 1–29.

Frutos, I., and Jażdżewska, A. M. (2019). Deep-sea amphipod fauna of the Sea of Okhotsk. *Prog. Oceanogr.* 178, 102147. doi: 10.1016/j.pocean.2019.102147

Gage, J. D., and Tyler, P. A. (1991). *Deep-Sea Biology: A Natural History of Organisms at the Deep-Sea Floor*. Cambridge: Cambridge University Press.

Garm, A., and Watling, L. (2013). "The crustacean integument: Setae, setules, and other ornamentation," in *The Natural History of the Crustacea. Volume 1 Functional Morphology and Diversity*, eds L. Watling and M. Thiel (Oxford: Oxford University Press), 167–198.

Golovan, O. A., Błażewicz, M., Brandt, A., Jażdżewska, A. M, Jóźwiak, P., Lavrenteva, A. V., et al. (2018). Diversity and distribution of peracarid crustaceans (Malacostraca) from the abyss adjacent to the Kuril-Kamchatka Trench. *Mar. Biodiver.* 49, 1343–1360. doi: 10.1007/s12526-018-0908-3

Hansen, H. J. (1913). Crustacea Malacostraca. *Danish Ingolf Expedition* 3, 1–145.

Jakiel, A., Palero, F., and Błażewicz, M. (2019). Deep ocean seascape and *Pseudotanaidae* (Crustacea: Tanaidacea) diversity at the Clarion-Clipperton Fracture Zone. *Sci. Rep.* 9:17305. doi: 10.1038/s41598-019-51434-z

Jakiel, A., Palero, F., and Błażewicz, M. (2020). Secrets from the deep: pseudotanaidae (Crustacea: Tanaidacea) diversity from the Kuril–Kamchatka Trench. *Prog. Oceanogr.* 183:102288. doi: 10.1016/j.pocean.2020.102288

Jóźwiak, P., and Jakiel, A. (2012). A new genus and new species of Agathotanaidae (Crustacea. Tanaidacea) from West Australia. *ZooKeys* 243, 15–26. doi: 10.3897/zookeys.243.3408

Kakui, K., and Kohtsuka, H. (2015). Two new shallow-water species of *Agathotanais* (Crustacea : Tanaidacea) from Japan. *Species Divers.* 20, 45–58. doi: 10.12782/sd.20.1.045

Katoh, K., and Standley, D. M. (2013). MAFFT multiple sequence alignment software version 7: improvements in performance and usability. *Mol. Biol. Evol.* 30, 772–780. doi: 10.1093/molbev/mst010

Kudinova-Pasternak, R. K. (1970). Tanaidacea of the Kurile-Kamchatka Trench. *Akademiya Nauk SSSR* 86, 341–380.

Kudinova-Pasternak, R. K. (1983). The abyssal Tanaidacea (Crustacea) of the Iberian and west-european hollows of the Atlantic Ocean. *Zool. Zhurnal.* 62, 1170–1176.

Kudinova-Pasternak, R. K. (1989). Tanaidacees abyssales (Crustacea, Tanaidacea) des parties nord-est et centrale de l'ocean Indien (d'apres des materiaux de l'expedition francaise "Safari-II"). 2. Sous-order Tanaidomorpha. *Zool. Zhurnal* 68, 27–40.

Kudinova-Pasternak, R. K. (1990). Tanaidacea from southeastern Atlantic Ocean and north of Elephant I. Trudy Instituta Okeanologii. *Akademiya Nauk SSSR* 126, 90–107.

Kumar, S., Stecher, G., Li, M., Knyaz, C., and Tamura, K. (2018). MEGA X: molecular evolutionary genetics analysis across computing platforms. *Battistuzzi FU (Ed). Mol. Biol. Evol.* 35, 1547–1549. doi: 10.1093/molbev/msy096

Lang, K. (1971). Die Gattungen *Agathotanais* Hansen Und *Paragathotanais* n. gen. (Tanaidacea). *Crustaceana* 21, 57–71. doi: 10.1163/156854071x00229

Larsen, K. (1999). Pacific Tanaidacea (Crustacea): revision of the genus *Agathotanais* with Description of Three New Species. *Rec. Aust. Mus.* 51, 99–112.

Larsen, K. (2005). *Deep-Sea Tanaidacea (Peracarida) From the Gulf of Mexico*. Leiden: Brill, doi: 10.1163/9789047416883

Larsen, K. (2007). Family Agathotanaidae Lang, 1971. *Zootaxa* 1599, 41–60.

Larsen, K., and Shimomura, M. (2007). Tanaidacea (Crustacea: Peracarida) from Japan III. The deep trenches: the Kurile-Kamchatka Trench and Japan Trench. *Zootaxa* 1599, 1–149.

Lörz, A. N., Jażdżewska, A. M., and Brandt, A. (2018). A new predator connecting the abyssal with the hadal in the Kuril-Kamchatka Trench. *NW Pacific. PeerJ* 6, e4887. doi: 10.7717/peerj.4887

Malyutina, M. V., Brandt, A., and Ivin, V. V. (2015). *The Russian-German Deep-Sea Expedition SokhoBio (Sea of Okhotsk Biodiversity Studies) to the Kurile Basin of the Sea of Okhotsk on Board of the R/V Akademik MA Lavrentyev. 71st Cruise, July 6th-August 6th, 2015. The Cruise Report. 1–103 (Report submitted to: Ministry of Education and Science (Russia) and Federal Ministry of Education and Research (Germany)*. Sofia: Ministry of Education and Science.

Nürnberg, D., and Tiedemann, R. (2004). Environmental change in the Sea of Okhotsk during the last 1.1 million year. *Paleoceanography* 19, A4011. doi: 10.1029/2004PA001023

O'Hara, T. D. (2019). The Eastern Australian Marine Parks: Biodiversity, Assemblage Structure, Diversity and Origin. Report to Parks Australia from

the National Environmental Science Program Marine Biodiversity Hub. Melbourne: Museum Victoria.

O'Hara, T. D., Williams, A., Althaus, F., Ross, A. S., and Bax, N. J. (2020a). Regional-scale patterns of deep seafloor biodiversity for conservation assessment. *Divers Distrib.* 26, 479–494. doi: 10.1111/ddi.13034

O'Hara, T. D., Williams, A., Ahyong, S. T., Alderslade, P., Alvestad, T., Bray, D., et al. (2020b). The lower bathyal and abyssal seafloor fauna of eastern Australia. *Mar. Biodivers. Rec.* 13:11. doi: 10.1186/s41200-020-00194-1

Pabis, K., Błażewicz-Paszkowycz, M., Jóźwiak, P., and Barnes, D. K. A. (2014). Tanaidacea of the Amundsen and Scotia seas: an unexplored diversity. *Antarct. Sci.* 27, 19–30. doi: 10.1017/s0954102014000303

Pabis, K., Jóźwiak, P., Lörz, A.-N. N., Schnabel, K. E., and Błażewicz-Paszkowycz, M. (2015). First insights into the deep-sea tanaidacean fauna of the Ross Sea: species richness and composition across the shelf break, slope and abyss. *Polar Biol.* 38, 1429–1437. doi: 10.1007/s00300-015-1706-z

Palero, F., Hall, S., Clark, P. F., Johnston, D., MacKenzie-Dodds, J., and Thatje, S. (2010). DNA extraction from formalin-fixed tissue: new light from the deep sea. *Sci. Mar.* 74, 465–470. doi: 10.3989/scimar.2010.74n3465

Rambaut, A., Drummond, A. J., Xie, D., Baele, G., and Suchard, M. A. (2018). Posterior summarization in Bayesian phylogenetics using Tracer 1.7. *Syst. Biol.* 67, 901–904. doi: 10.1093/sysbio/syy032

Riehl, T., Brenken, N., Brix, S., Driskell, A., Kaiser, S., and Brandt, A. (2014). Field and laboratory methods for DNA studies on deep-sea isopod crustaceans. *Pol. Polar Res.* 35, 203–224.

Saeedi, H., and Brandt, A. (2020). *Biogeographic Atlas of the Deep NW Pacific Fauna*. Electronic publication: Pensoft. doi: 10.3897/ab.e51315.

Schofield, C. (2018). "Exploring the deep frontier," in *Global Commons and the Law of the Sea*, ed. K. Zou (Leiden: Brill), 151–167. doi: 10.1163/9789004373334_010

Sieg, J. (1986). *Tanaidacea (Crustacea) von der Antartiks und Subantarktis. II. Tanaidacea gesammelt von Dr. J. W. Wägele während der Deutschen Antarktis Expedition 1983*. Kiel: Mitteilungen aus dem Zoologischen Museum der Universität Kiel, 1–80.

Stępień, A., Pabis, P., and Błażewicz, M. (2019). Tanaidacean faunas of the sea of okhotsk and northern slope of the Kuril-Kamchatka Trench. *Prog. Oceanogr.* 178:102196. doi: 10.1016/j.pocean.2019.102196

Sweetman, A. K., Thurber, A. R., Smith, C. R., Levin, L. A., Mora, C., Wei, C., et al. (2017). Major impacts of climate change on deep-sea benthic ecosystems. *Elementa Sci. Anthrop.* 5, 4. doi: 10.1525/elementa.203

Washburn, T. W., Menot, L., Bonifácio, P., Pape, E., Błażewicz, M., Bribiesca-Contreras, G., et al. (2021). Patterns of macrofaunal biodiversity across the clarion-clipperton zone: an area targeted for seabed mining. *Front. Mar. Sci.* 8:626571. doi: 10.3389/fmars.2021.626571

Woolley, S. N. C., Tittensor, D. P., Dunstan, P. K., Guillera-Arroita, G., Lahoz-Monfort, J. J., Wintle, B. A., et al. (2016). Deep-sea diversity patterns are shaped by energy availability. *Nature* 533, 393–396. doi: 10.1038/nature 17937

Conflict of Interest: The authors declare that the research was conducted in the absence of any commercial or financial relationships that could be construed as a potential conflict of interest.

Publisher's Note: All claims expressed in this article are solely those of the authors and do not necessarily represent those of their affiliated organizations, or those of the publisher, the editors and the reviewers. Any product that may be evaluated in this article, or claim that may be made by its manufacturer, is not guaranteed or endorsed by the publisher.